Supporting Information for

Asymmetric photoenzymatic synthesis of chiral γ-acyloxybutenolides from 2-furoic acid in 2-methyltetrahydrofuran: from batch to flow processs

Yi He, and Ning Li*

School of Food Science and Engineering, South China University of Technology, Guangzhou 510640, China

* Corresponding author. E-mail: lining@scut.edu.cn

Materials

HB (98%) was purchased from Macklin Biochemical Technology Co., Ltd. (Shanghai, China). FCA (98%), 2-MeTHF (99%), ViOAc (99%), vinyl butyrate (99%), vinyl hexanoate (99%), vinyl octanoate (99%), vinyl decanoate (99%), vinyl laurate (99%), vinyl benzoate(99%), vinyl cinnamate (99%), vinyl methacrylate (98%), vinyl pivalate (99%), and 2,2,6,6-tetramethylpiperidine (TEMP, >98%) were obtained from Aladdin Biochemical Technology Co., Ltd. (Shanghai, China). TCPP (97%) was purchased from Chemsoon Co., Ltd. (Shanghai, China). Oxygen (O_2, ≥99.5%) was obtained from Guangzhou Shengying Chemical Co., Ltd. (Guangzhou, China). N,N-Diethylformamide (DEF) was purchased from Bide Pharmatech Technology Co., Ltd. (Shanghai, China). $ZrCl_4$ was purchased from Adamas-beta Co., Ltd. (Shanghai, China). Other chemicals were commercially available. Novozym 435 (*Candida antarctica* lipase B immobilized on a macroporous acrylic resin), Lipozyme TL IM (*Thermomyces lanuginosus* lipase immobilized on silica gel), Lipozyme RM IM (*Rhizomucor miehei* lipase immobilized on a macroporous acrylic resin), Lipura Select (*Rhizomucor miehei* lipase immobilized on a new carrier), Lipura Flex (*Candida antarctica* lipase B immobilized on a new carrier) were from Novozymes Co., Ltd. (China). Lipase AK (from *Pseudomonas fluorescens*) is a gift from Amano (Japan).

HPLC analysis

For determining the conversions and yields, the reaction mixtures were analyzed on a Zorbax Eclipse Plus C18 column (4.6 mm × 250 mm, 5 μm, Agilent, USA) by using a reversed phase HPLC equipped with a Waters 996 photodiode array detector (Waters, USA). The quantitative analyses for FCA (wavelength: 250 nm, retention time: 5.2 min), HB (210 nm, 4.2 min) and **4a** (210 nm, 6.4 min) were performed with the mixture of acetonitrile/0.02%

phosphoric acid aqueous solution (4/6, v/v) as the mobile phase. The column temperature and flow rate were 35 °C and 0.6 mL/min, respectively.

Products (**4b-j**) were analyzed using Titank C18 column (4.6 mm × 250 mm, 5 μm, Phenomenex, USA) and Waters 2489 UV/visible light detector (Waters, USA). The flow rate was 0.6 mL/min, and the column temperature was 30 °C. The mixture of acetonitrile/deionized water (8/2, v/v) was used as the mobile phase for quantifying **4b** (210 nm, 5.8 min), **4c** (210 nm, 7.1 min), **4d** (210 nm, 9.4 min), **4e** (210 nm, 14.1 min), **4f** (210 nm, 23.2 min), **4g** (210 nm, 6.3 min), **4h** (210 nm, 5.7 min), **4i** (233 nm, 6.1 min), and **4j** (276 nm, 6.6 min).

For determining the product ee values, the isolated products or the reaction mixtures containing the products were analyzed by an Agilent 1100 HPLC equipped with a UV-visible light detector (Agilent, USA). Detailed HPLC methods were shown in Table S1.

Table S1. Chiral HPLC analysis

Product	Mobile phase	Column	Flow rate (mL/min)	Detection wavelength (nm)
4a	*n*-hexane: isopropanol (95/5, v/v)	CHIRALPAK® AD-H (4.6 mm × 150 mm, 5 μm, Daicel Corporation, Japan)	1.0	210
4b	*n*-hexane: isopropanol (90/10, v/v)	CHIRALPAK® AD-H (4.6 mm × 250 mm, 5 μm, Daicel Corporation, Japan)	1.0	210
4c	*n*-hexane: isopropanol (98/2, v/v)	CHIRALPAK® AD-H (4.6 mm × 250 mm, 5 μm, Daicel Corporation, Japan)	0.8	210
4d	*n*-hexane: isopropanol (98/2, v/v)	CHIRALPAK® AD-H (4.6 mm × 250 mm, 5 μm, Daicel Corporation, Japan)	0.8	210
4e	*n*-hexane: isopropanol (98/2, v/v)	CHIRALPAK® AD-H (4.6 mm × 250 mm, 5 μm, Daicel Corporation, Japan)	0.8	210
4f	*n*-hexane: isopropanol (98/2, v/v)	CHIRALPAK® AD-H (4.6 mm × 250 mm, 5 μm, Daicel Corporation, Japan)	0.8	210
4g	*n*-hexane: isopropanol (95/5, v/v)	CHIRALPAK® AD-H (4.6 mm × 250 mm, 5 μm, Daicel Corporation, Japan)	1.0	210
4h	*n*-hexane: isopropanol (92/8, v/v)	CHIRALPAK® AD-H (4.6 mm × 250 mm, 5 μm, Daicel Corporation, Japan)	1.0	210
4i	*n*-hexane: isopropanol (95/5, v/v)	CHIRALCEL® OD-H (4.6 mm × 250 mm, 5 μm, Daicel Corporation, Japan)	1.0	233
4j	*n*-hexane: isopropanol (85/15, v/v)	CHIRALPAK® AD-H (4.6 mm × 250 mm, 5 μm, Daicel Corporation, Japan)	1.0	276

One-pot concurrent synthesis of ABs.

To a 20-mL vial were added 4.5 mL 2-MeTHF, 0.5 mL vinyl ester, 50 mM FCA, 50 g/L Lipozyme TL IM, and 1 mM TCPP, followed by reaction at 500 rpm and 30 °C under irradiation by 30 W green LEDs (530-540 nm). After 12h, the enzyme was filtered off, and the filtrate was concentrated under vacuum. The residue was subjected to flash column chromatography using petroleum ether (PE)/ethyl acetate (EA) as the mobile phase. The products isolated were characterized by ^{1}H NMR (Bruker Avance Neo 500M NMR spectrometer, Germany) and ^{13}C NMR (Bruker Avance III HD 600 NMR spectrometer, Germany). The NMR spectra are presented below.

γ-Acetoxybutenolide (4a)

Colorless oil. **^{1}H NMR (500 MHz, $CDCl_3$) δ** 7.32 (d, *J* = 5.7 Hz, 1H), 6.99 (s, 1H), 6.31 (d, *J* = 5.6 Hz, 1H), 2.16 (s, 3H). **^{13}C NMR (151 MHz, $CDCl_3$) δ** 169.62, 168.88, 149.72, 125.20, 93.80, 20.63. The data are the same as the previous results.[1, 2]

γ-Butyryloxybutenolide (4b)

Colorless oil. **^{1}H NMR (500 MHz, $CDCl_3$) δ** 7.32 (dd, *J* = 5.7, 1.4 Hz, 1H), 7.01 (t, *J* = 1.3 Hz, 1H), 6.31 (dd, *J* = 5.6, 1.2 Hz, 1H), 2.38 (td, *J* = 7.3, 1.8 Hz, 2H), 1.69 (q, *J* = 7.4 Hz, 2H), 0.97 (t, *J* = 7.4 Hz, 3H). **^{13}C NMR (151 MHz, $CDCl_3$) δ** 171.57, 169.72, 149.85, 125.15, 93.74, 35.66, 18.00, 13.50. The data are the same as the previous results.[2]

γ-Caproyloxybutenolide (4c)

Colorless oil. **^{1}H NMR (500 MHz, $CDCl_3$) δ** 7.34 (dd, *J* = 5.7, 1.4 Hz, 1H), 7.03 (d, *J* = 1.5 Hz, 1H), 6.33 (dd, *J* = 5.6, 1.2 Hz, 1H), 2.42 (td, *J* = 7.4, 1.3 Hz, 2H), 1.68 (dd, *J* = 8.6, 6.1 Hz, 2H), 1.34 (dq, *J* = 7.2, 3.5 Hz, 4H), 0.94 – 0.90 (m, 3H). **^{13}C NMR (151 MHz, $CDCl_3$) δ** 171.76, 169.72, 149.83, 125.16, 93.76, 33.82, 31.09, 24.15, 22.22, 13.84.

HRMS (ESI$^+$): calcd. for $C_{10}H_{14}O_4$ $[M+Na]^+$: 221.0790, found: 221.0796.

γ-Octanoyloxybutenolide (4d)

Colorless oil. **^{1}H NMR (500 MHz, $CDCl_3$) δ** 7.31 (dd, *J* = 5.7, 1.3 Hz, 1H), 7.03 – 6.98 (m, 1H), 6.31 (dd, *J* = 5.6, 1.1 Hz, 1H), 2.39 (td, *J* = 7.4, 1.3 Hz, 2H), 1.64 (d, *J* = 7.5 Hz, 2H), 1.33 – 1.24 (m, 8H), 0.90 – 0.86 (m, 3H). **^{13}C NMR (151 MHz, $CDCl_3$) δ** 171.76, 169.69, 149.78, 125.18, 93.76, 33.87, 31.57, 28.91, 28.82, 24.48, 22.57, 14.04.

HRMS (ESI$^+$): calcd. for $C_{12}H_{18}O_4$ $[M+H]^+$: 227.1283, found: 227.1287.

γ-Capryloxybutenolide (4e)

Colorless oil. **^{1}H NMR (500 MHz, $CDCl_3$) δ** 7.31 (d, *J* = 5.8 Hz, 1H), 7.01 (s, 1H), 6.31 (d, *J* = 5.6 Hz, 1H), 2.39 (dd, *J* = 8.4, 6.7 Hz, 2H), 1.64 (d, *J* = 7.5 Hz, 2H), 1.29 – 1.22 (m, 13H), 0.88 (t, *J* = 6.8 Hz, 4H). **^{13}C NMR (151 MHz, $CDCl_3$) δ** 171.76, 169.69, 149.79, 125.17, 93.77, 33.90, 33.86, 31.84, 29.39, 29.34, 29.24, 29.22, 29.17, 29.06, 28.96, 24.70, 24.48, 22.65, 14.10.

HRMS (ESI$^+$): calcd. for $C_{14}H_{22}O_4$ $[M+Na]^+$: 277.1416, found: 277.1407.

γ-Lauroyloxybutenolide (4f)

White solid. **^{1}H NMR (500 MHz, $CDCl_3$) δ** 7.31 (dd, *J* = 5.8, 1.2 Hz, 1H), 7.02 (s, 1H), 6.31 (d, *J* = 5.6 Hz, 1H), 2.43 – 2.37 (m, 2H), 1.68 – 1.62 (m, 2H), 1.27 (m, *J* = 8.5 Hz, 16H), 0.88 (t, *J* = 6.8 Hz, 3H). **^{13}C NMR (151 MHz, $CDCl_3$) δ**

171.75, 169.69, 149.81, 125.16, 93.76, 33.86, 31.90, 29.58, 29.56, 29.39, 29.32, 29.17, 28.96, 24.47, 22.68, 14.11. The data are the same as the previous results.[1]

γ-Pivaloyloxybutenolide (4g)

Pale yellow oil. **^{1}H NMR (500 MHz, $CDCl_3$) δ** 7.33 (d, *J* = 5.7 Hz, 1H), 6.99 (s, 1H), 6.31 (d, *J* = 5.7 Hz, 1H), 1.23 (s, 9H). **^{13}C NMR (151 MHz, $CDCl_3$) δ** 176.48, 169.79, 149.90, 125.18, 94.04, 38.96, 27.18, 26.84. The data are the same as the previous results.[1]

γ-Methacryloyloxybutenolide (4h)

White solid. **^{1}H NMR (500 MHz, $CDCl_3$) δ** 7.37 (dd, *J* = 5.7, 1.3 Hz, 1H), 7.06 (d, *J* = 1.4 Hz, 1H), 6.33 (dd, *J* = 5.6, 1.2 Hz, 1H), 6.20 (d, *J* = 1.1 Hz, 1H), 5.73 (t, *J* = 1.5 Hz, 1H), 1.97 (t, *J* = 1.3 Hz, 3H). **^{13}C NMR (151 MHz, $CDCl_3$) δ** 169.68, 165.11, 149.84, 134.73, 128.41, 125.27, 94.30, 18.08.

γ-Benzoyloxybutenolide (4i)

White solid. **^{1}H NMR (500 MHz, $CDCl_3$) δ** 8.01 – 7.95 (d, 2H), 7.60 – 7.53 (t, 1H), 7.44 – 7.38 (m, 3H), 7.19 (s, *J* = 1.5 Hz, 1H), 6.32 (dd, *J* = 5.6, 1.1 Hz, 1H). **^{13}C NMR (151 MHz, $CDCl_3$) δ** 169.70, 164.57, 149.88, 134.20, 130.16, 128.68, 128.16, 125.39, 94.49. The data are the same as the previous results.[1]

γ-Cinnamoyloxybutenolide (4j)

White solid. **^{1}H NMR (500 MHz, $CDCl_3$) δ** 7.80 (d, *J* = 16.0 Hz, 1H), 7.56 – 7.53 (m, 2H), 7.43 – 7.40 (m, 4H), 7.15 (d, *J* = 1.3 Hz, 1H), 6.44 (d, *J* = 16.0 Hz, 1H), 6.36 (dd, *J* = 5.6, 1.2 Hz, 1H). **^{13}C NMR (151 MHz, $CDCl_3$) δ** 169.72, 164.68, 149.88, 147.92, 131.14, 129.07, 128.44, 125.28, 115.72, 94.14.

HRMS (ESI^+): calcd. for $C_{13}H_{10}O_4$ $[M+Na]^+$: 253.0477, found: 253.0475.

Preparation of PCN-222 and other MOFs

PCN-222, PCN-224, ZPM, and UiO-4 were prepared according to the previous reports,[3-6] with the slight modifications. For the synthesis of PCN-222, briefly, $ZrCl_4$ (225 mg), TCPP (150 mg) and benzoic acid (8100 mg) were ultrasonically dissolved in 24 mL of DEF in a 100 mL Pyrex vial. The mixture was heated at 120 °C for 48 h. After cooling down to room temperature, deep purple solid was harvested by filtration.

EPR detection of $^1O_2$

The suspension of PCN-222 (1 mg/mL) in 1 mL deionized H_2O was mixed with 5 μL TEMP (approximately 30 mM of the final concentration). The mixture was irradiated under open air conditions by a 300 W Xenon lamp for 10 min, followed by EPR measurement (Bruker EMXplus EPR spectrometer, German) under the magnetic field range of 3460-3560 G, microwave frequency of 9.853 GHz, microwave power of 20 mW, and modulation amplitude of 1 G. The mixture operated under dark conditions serve as the control.

Flow photooxygenation of FCA into HB by PCN-222

The modules are interconnected with polytetrafluoroethylene (PTFE) tubes (internal diameters: 1 mm; external

diameters: 3 mm) and peristaltic pump tubing to form the final flow system. PTFE tubes exhibit excellent corrosion resistance to organic solvents and are capable of undergoing photo-oxidation reactions.

To the 250 mL glass bottle was added 60 mL of 2-MeTHF containing 0.5 M FCA. Non-woven fabric (with an individual area of about 2 × 10 cm^2) deposited with approximately 80 mg of catalyst was packed into 8 quartz tubes (internal diameters: 8 mm; length: 120 mm). These quartz tubes were then connected to a tubular reactor with a total volume of approximately 50 mL. The reaction mixture was bubbled with O_2 for 25 minutes. A O_2 balloon was then installed and connected to the tubular reactor via a peristaltic pump. O_2 was then purged into the reaction system by excluding and charging with O_2 several times. Then two peristaltic pumps were respectively loaded with two tubes, one for oxygen supply (5 mL/min) and the other for circulating the reaction mixture (5 mL/min); these two tubes are connected to a single tube via a Y-mixer. The quartz tubes were irradiated under White LEDs (30 W, 400-850 nm) at 30 °C. Aliquots were withdrawn at specified time intervals from the reaction mixtures, and then diluted with the corresponding mobile phase prior to HPLC analysis. All the experiments were conducted at least in duplicate, and all the data were the averages of experimental results. The yields and conversions were determined by HPLC, based on the corresponding calibration curves.

Batch photooxygenation of FCA into HB by PCN-222

To a 100 mL Schlenk tube were added 60 mL 2-MeTHF, 50 mM FCA, and 80 mg of PCN-222; then, the mixture was bubbled with O_2 for 25 minutes, followed by irradiation under white LEDs (30 W, 400-850 nm) at 30 °C and 500 rpm to undergo the photooxidation reaction. Aliquots were withdrawn at specified time intervals from the reaction mixtures, and then diluted with the corresponding mobile phase prior to HPLC analysis. All the experiments were conducted at least in duplicate, and all the data were the averages of experimental results. The yields and conversions were determined by HPLC, based on the corresponding calibration curves.

One-pot two-step photoenzymatic synthesis of 4a from FCA via a flow process

Upon the flow photooxygenation of FCA, 15 mL of ViOAc was supplemented into the reaction mixture. Then, the reaction mixture stored in the glass bottle was introduce into the immobilized enzyme packed-bed reactor (internal diameters: 1.0 cm; length: 20 cm, loaded with around 7 g of Lipozyme TL IM) by tuning the three-way valve. The enzyme reactor was continuously heated to around 50 ℃ by using an electric heating sleeve. The reaction mixture was circulated within the tubular system via a peristaltic pump (10 mL/min). Aliquots were withdrawn at specified time intervals from the reaction mixture for HPLC analysis.

Gram-scale preparation of 4a

After the flow synthesis **4a** at 0.5 M substrate loading, the reaction mixture was concentrated under vacuum. The residue was subjected to flash silica column chromatography (PE/EA = 3:1, v/v), affording **4a** (3.67 g, 86% isolated yield) as colorless oil. Its ^{1}H NMR spectrum is shown in Fig. S14.

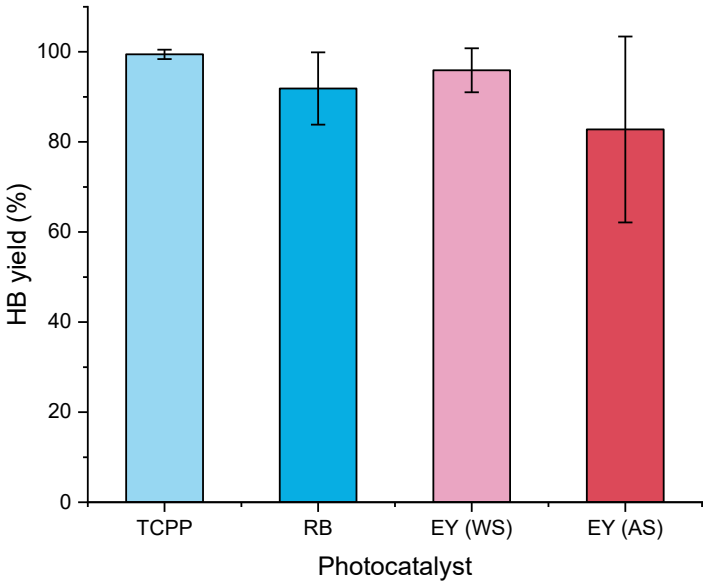

Fig. S1. Photooxygenation of FCA by different photocatalysts. Reaction conditions: 100 mM FCA, 2 mol% catalyst, 30 W green LEDs (530-540 nm), 2 mL 2-MeTHF, 30 ℃, air, 500 rpm, 12 h. RB, rose bengal; EY (WS), water-soluble eosin Y; EY (AS), alcohol-soluble eosin Y.

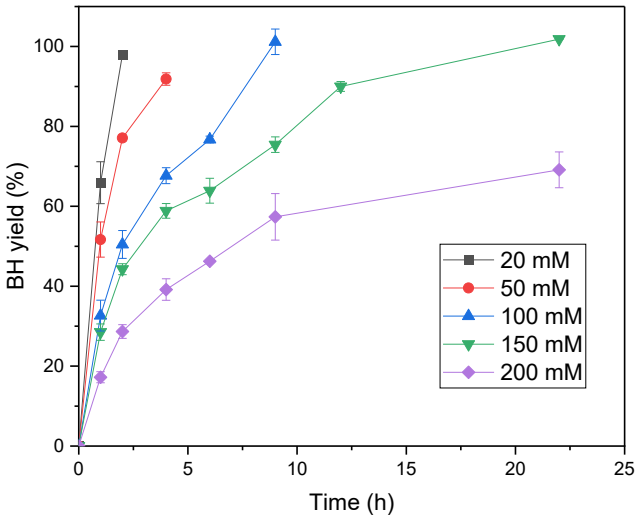

Fig. S2. Effect of substrate concentrations on photocatalytic synthesis of HB. Reaction conditions: 20-200 mM FCA, 2 mol% TCPP, 2 mL 2-MeTHF, 30 W green LEDs (530-540 nm), air, 30 °C, 500 rpm.

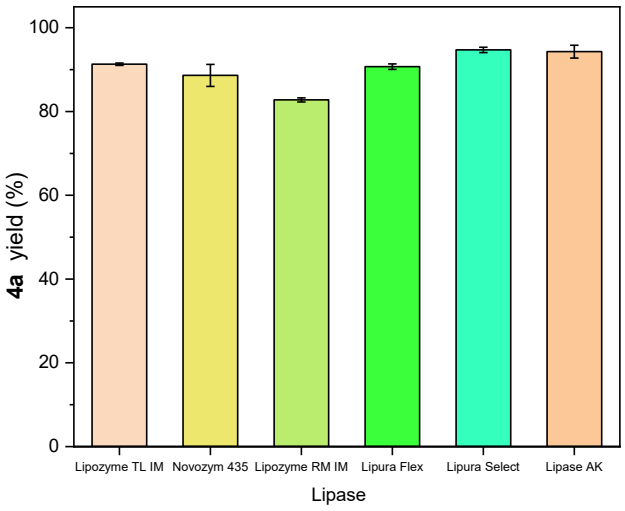

Fig. S3. Synthesis of **4a** catalyzed by various lipases. Reaction conditions are the same as those in Fig. 1C, with the exception of the reaction period of 18 h.

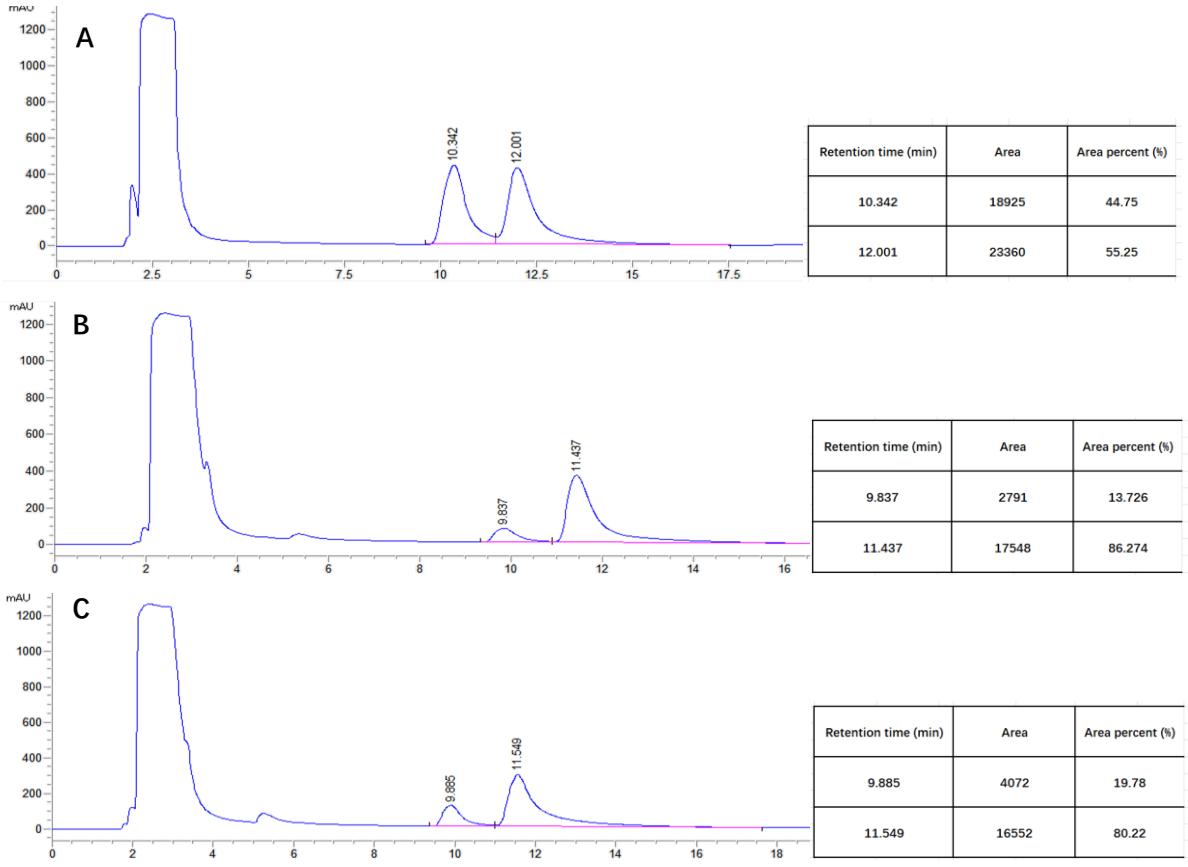

Retention time (min)	Area	Area percent (%)
10.342	18925	44.75
12.001	23360	55.25

Retention time (min)	Area	Area percent (%)
9.837	2791	13.726
11.437	17548	86.274

Retention time (min)	Area	Area percent (%)
9.885	4072	19.78
11.549	16552	80.22

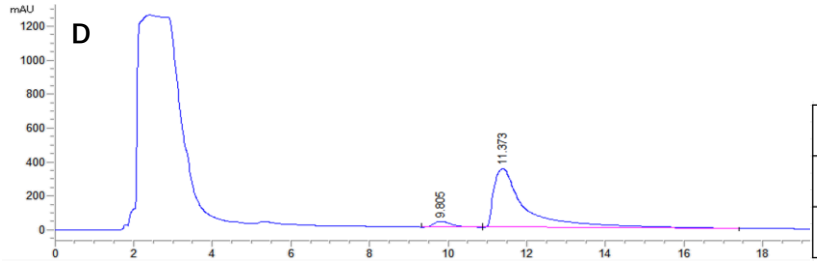

Retention time (min)	Area	Area percent (%)
9.805	1105	5.24
11.373	19998	94.76

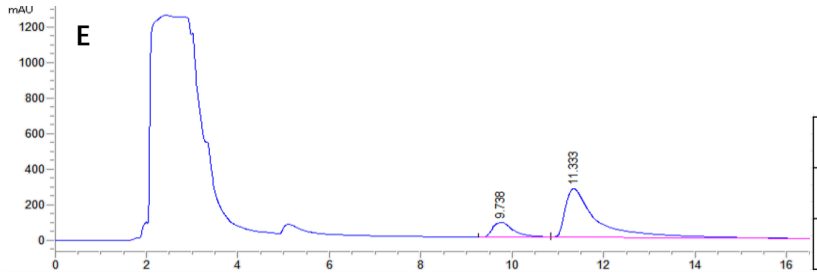

Retention time (min)	Area	Area percent (%)
9.738	2784	16.65
11.333	13932	83.35

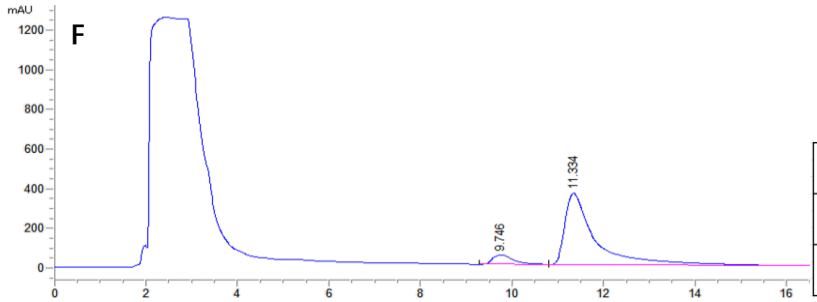

Retention time (min)	Area	Area percent (%)
9.746	1532	8.26
11.334	17018	91.74

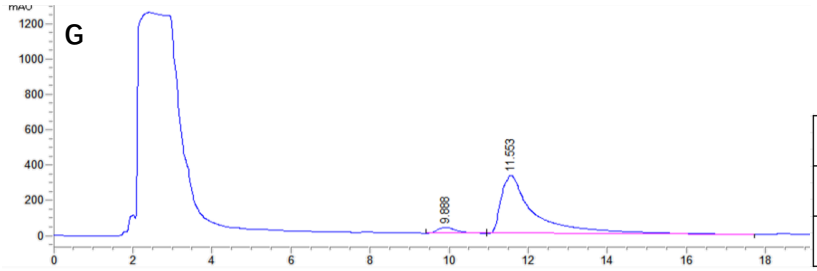

Retention time (min)	Area	Area percent (%)
9.888	1114	5.33
11.553	19779	94.67

Fig. S4. Chiral HPLC analysis of the product obtained by chemical acylation (A), Lipozyme TL IM (B), Novozym 435 (C), Lipozyme RM IM (D), Lipura Flex (E), Lipura Select (F), and lipase AK (G).

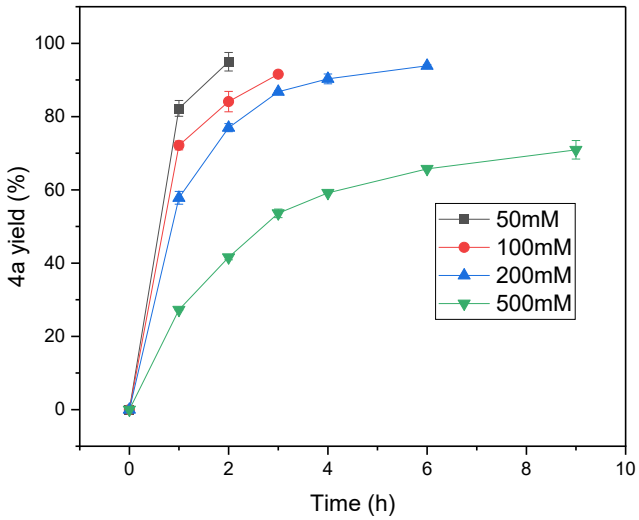

Fig. S5. Effect of substrate concentrations on enzymatic acylation of HB by Lipozyme TL IM. Reaction conditions: 50-500 mM HB, 50 g/L Lipozyme TL IM, 2 mL 2-MeTHF containing 10% (v/v) ViOAc, 220 rpm, 50 ℃.

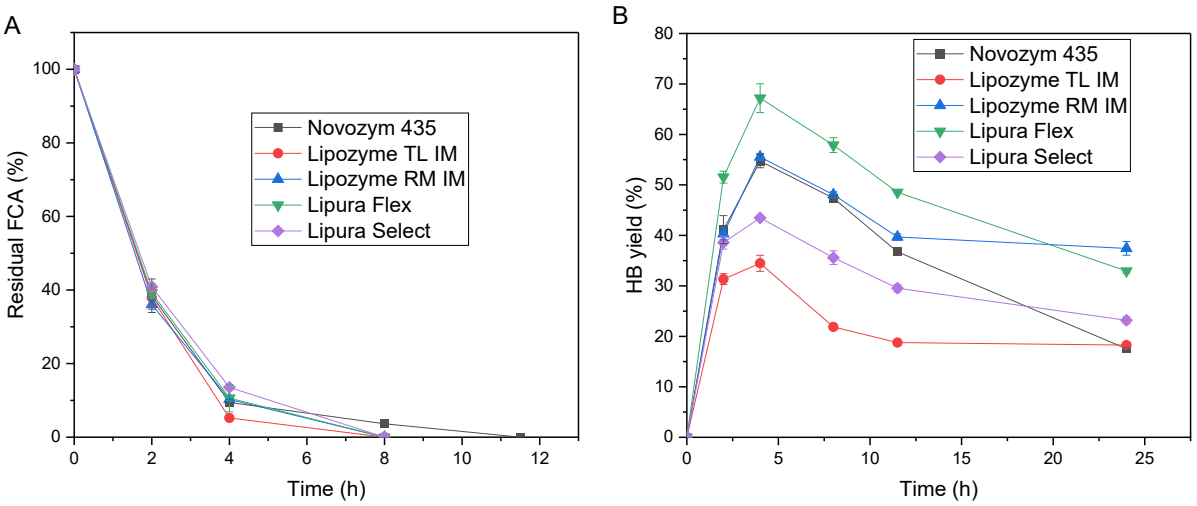

Fig. S6. One-pot concurrent conversion of FCA into **4a**: (A) FCA consumption; (B) HB transformation. Reaction conditions are the same as those described in Fig. 2.

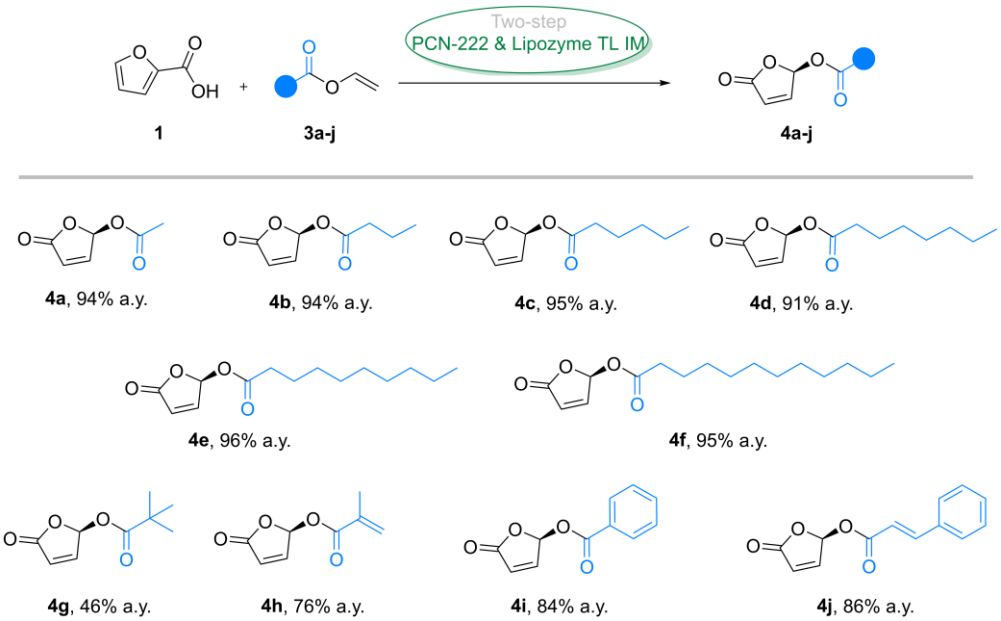

Fig. S7. One-pot two-step conversion of FCA into **4a-j**. Reaction conditions: 50 mM FCA, 2 mg PCN-222, 1.8 mL 2-MeTHF, 30 W white LEDs (400-830 nm), O_2, 30 °C, 500 rpm; after 1 h, adding 50 g/L Lipozyme TL IM and 200 μL vinyl ester, reaction at 50 °C and 220 rpm, 6 h, analytic yield (a.y.).

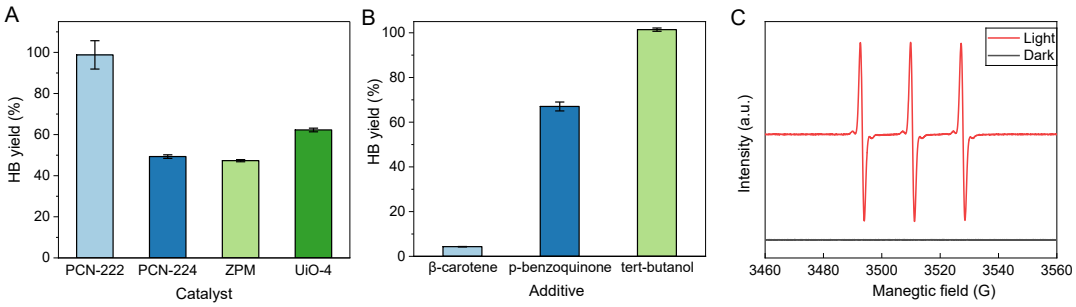

Fig. S8. Photooxygenation of FCA by MOF-based photocatalysts: (A) comparison of the catalytic performances of MOF-based photocatalysts; (B) effect of ROS scavengers on FCA photooxygenation; (C) EPR spectra for the detection of $^1O_2$. Reaction conditions: (A) 50 mM FCA, 2 mg photocatalyst, 2 mL 2-MeTHF, 30 W white LEDs (400-830 nm), O_2, 30 °C, 500 rpm, 1 h; (B) the conditions are the same as those of (A), except for the addition of extra additives.

To identify the primary ROS involved in PCN-222-mediated photooxygenation of FCA, a series of scavenging experiments was conducted. As shown in Fig. S7B, the HB yield decreased sharply to less than 5% when β-carotene, a scavenger for $^1O_2$, was added, indicating that $^1O_2$ plays a dominant role in the photooxygenation. In contrast, the addition of *p*-benzoquinone (for scavenging superoxide anions, $O_2\cdot^-$) and *tert*-butanol (for trapping hydroxyl radicals, ·OH) resulted in moderate and marginal decreases in HB yields, respectively. These findings indicate that

$O_2 \cdot^-$ as well as ·OH plays a minor role in the photochemical oxidation. To directly verify the generation of $^1O_2$ during photooxygenation, electron paramagnetic resonance (EPR) coupled with a $^1O_2$ detector probe, 2,2,6,6-tetramethylpiperidine (TEMP), was used, since TEMP reacts with $^1O_2$ to produce a stable nitroxide radical, 2,2,6,6-tetramethylpiperidine-1-oxyl (TEMPO), which can be quantified by EPR.[7, 8] As shown in Fig. S7C, the mixture of PCN-222 and TEMP provided a 1: 1: 1 triplet peak upon irradiation for 10 min with a 300 W Xenon lamp (λ>420 nm), corresponding to the signal of TEMPO.[5] However, no significant radical signal was observed under dark conditions. The results demonstrate that the oxidation of FCA majorly stems from the generation of $^1O_2$.

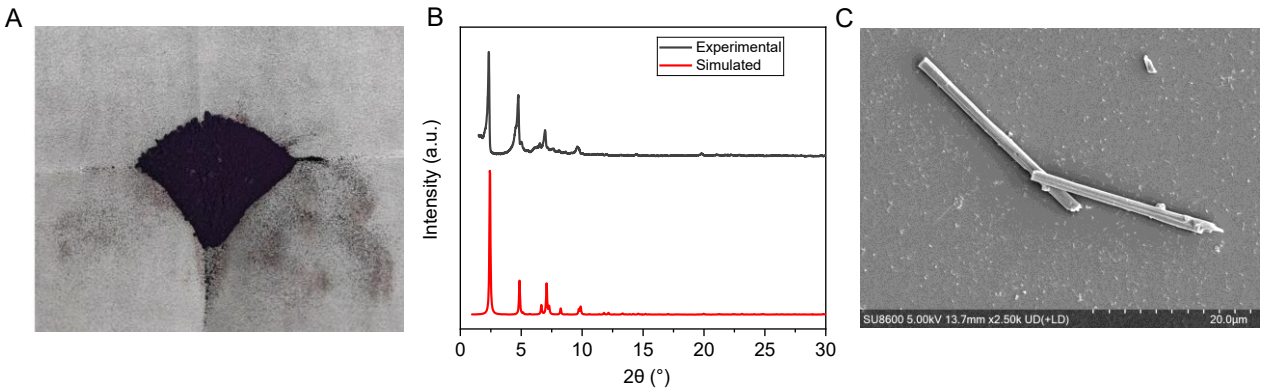

Fig. S9. (A) The image of PCN-222; (B) PXRD pattern of PCN-222; (C) SEM image of PCN-222

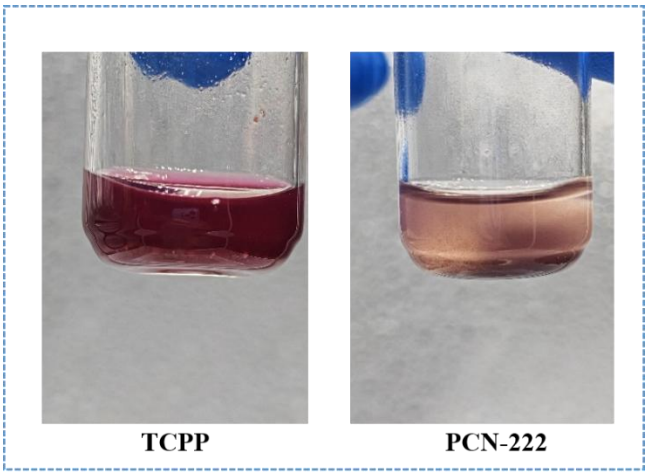

Fig. S10. The images of TCPP and PCN-222 dispersed in 2-MeTHF.

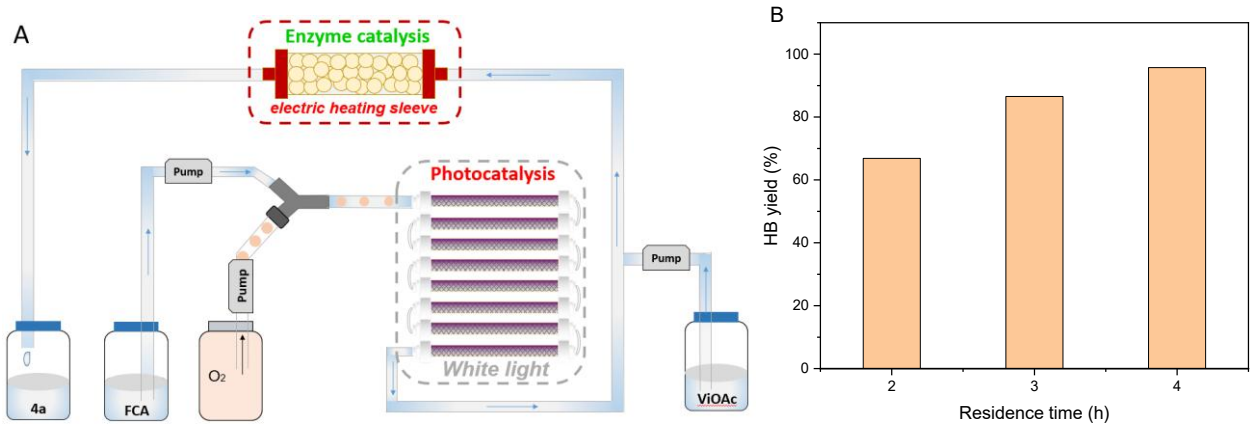

Fig. S11. Continuous photoenzymatic synthesis of **4a**: (A) the set-up diagram; (B) effect of the residence times on HB synthesis. Reaction conditions: 50 mM FCA, 80 mg PCN-222, 60 mL 2-MeTHF, 30 W white LEDs (400-830 nm), 30 °C, 0.25-0.5 mL/min reaction mixture, 5 mL/min O_2.

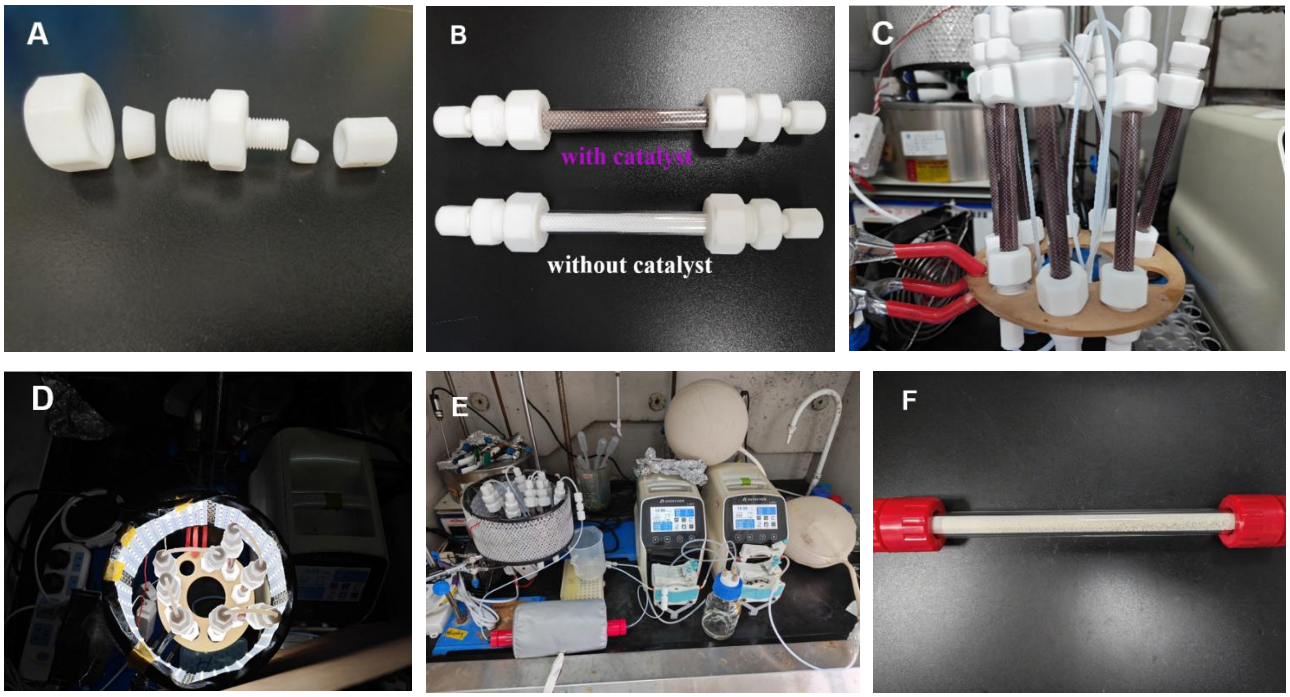

Fig. S12. Pictures of the connectors (A); photoreactors loaded with or without catalyst (B); front view of the photoreactors (C); top view of the photoreactors (D); experimental set-up of the flow tubular system (E); front view of the enzymatic reactor (F).

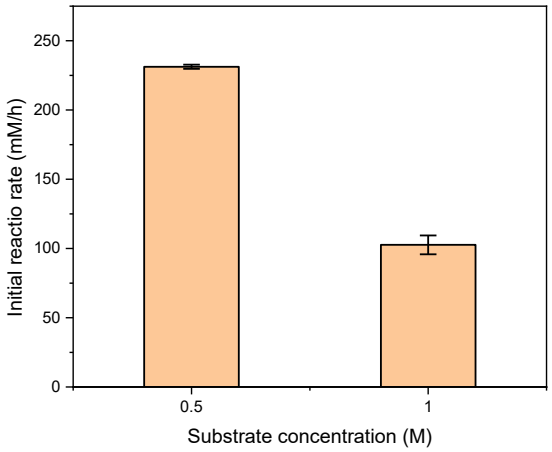

Fig. S13. Inhibition of HB toward Lipozyme TL IM. The data were pulled up from Fig. 8 (at 1 h).

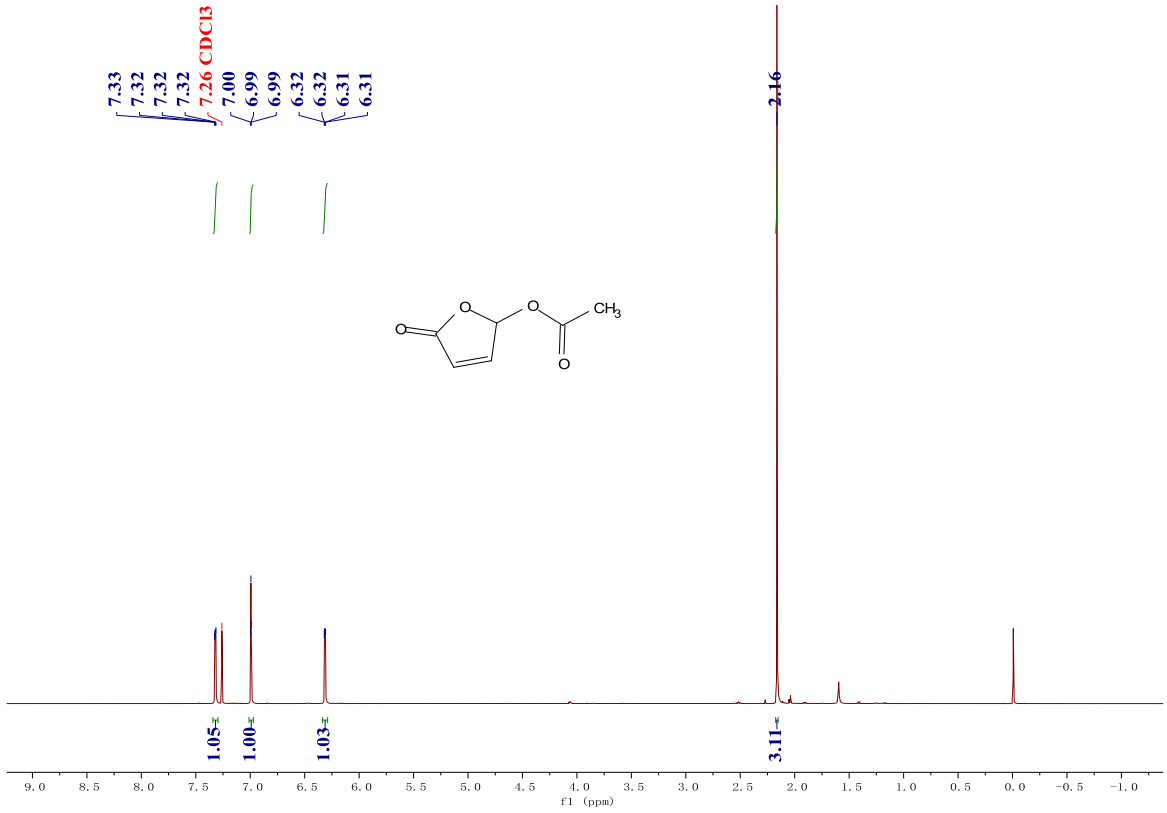

Fig. S14. ^{1}H NMR spectrum of **4a** isolated in gram-scale synthesis (600 MHz, $CDCl_3$).

Table S2. Estimation of waste generated in preparative-scale synthesis of **4a** at 0.5 M substrate loading without considering purification.

Component	E-factor contribution
Lipozyme TL IM	1.79
PCN-222	0.02
ViOAc[a]	2.95
2-MeTHF	13.16
Sum	17.9

[a]: including unreacted ViOAc, and generated by-products acetic acid and acetaldehyde.

NMR spectra

Fig. S15. ^{1}H NMR spectrum of **4a** (500 MHz, $CDCl_3$)

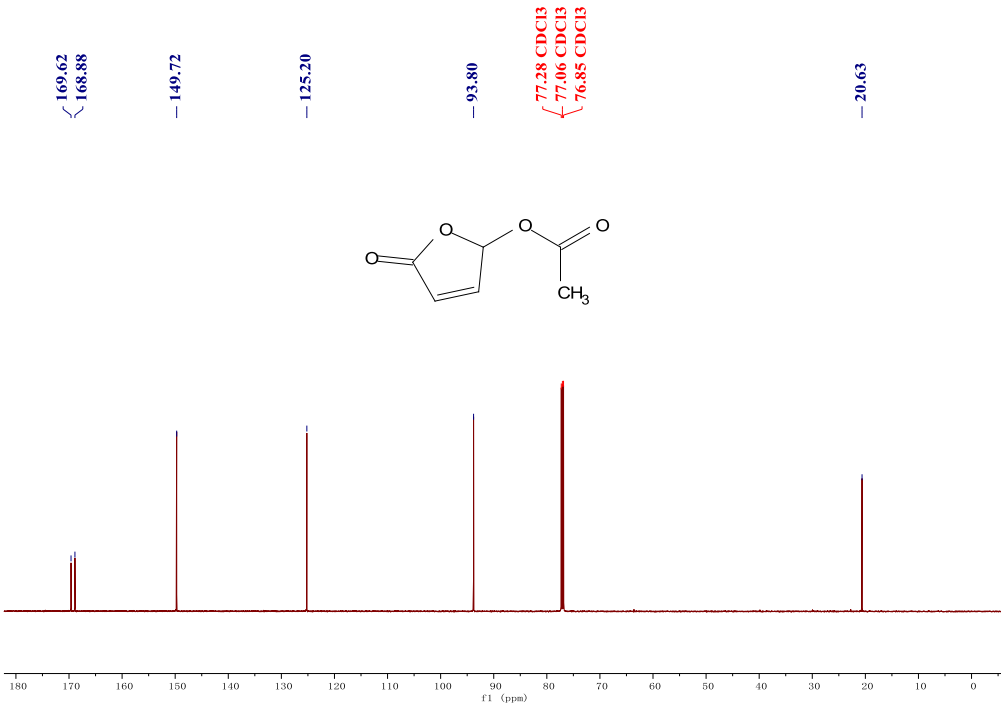

Fig. S16. ^{13}C NMR spectrum of **4a** (151 MHz, $CDCl_3$)

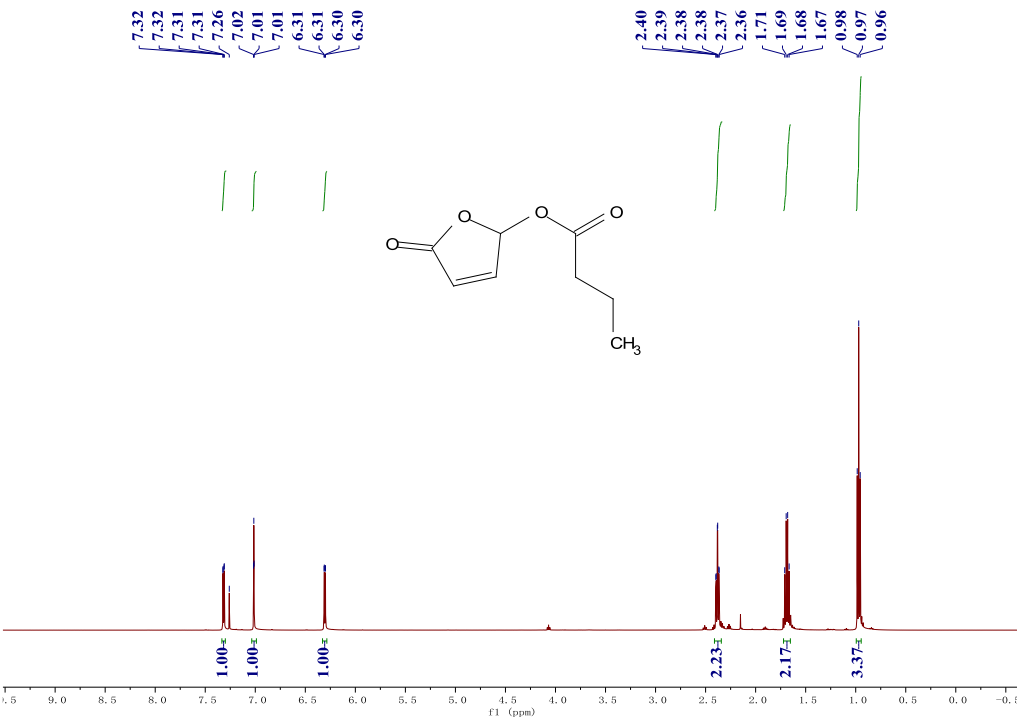

Fig. S17. ^{1}H NMR spectrum of **4b** (500 MHz, $CDCl_3$)

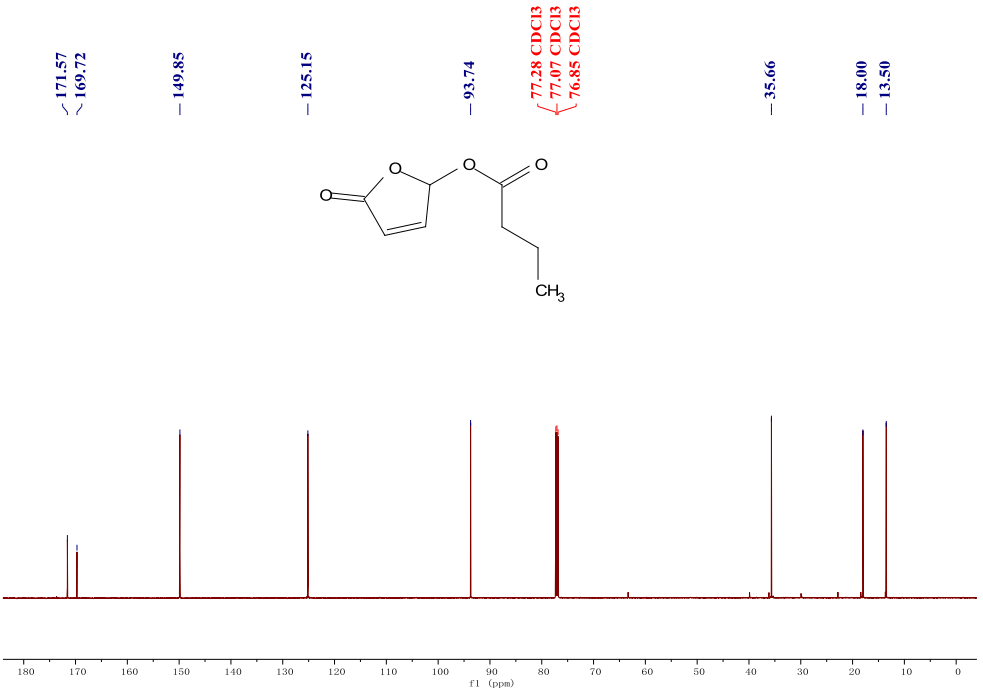

Fig. S18. ^{13}C NMR spectrum of **4b** (151 MHz, $CDCl_3$)

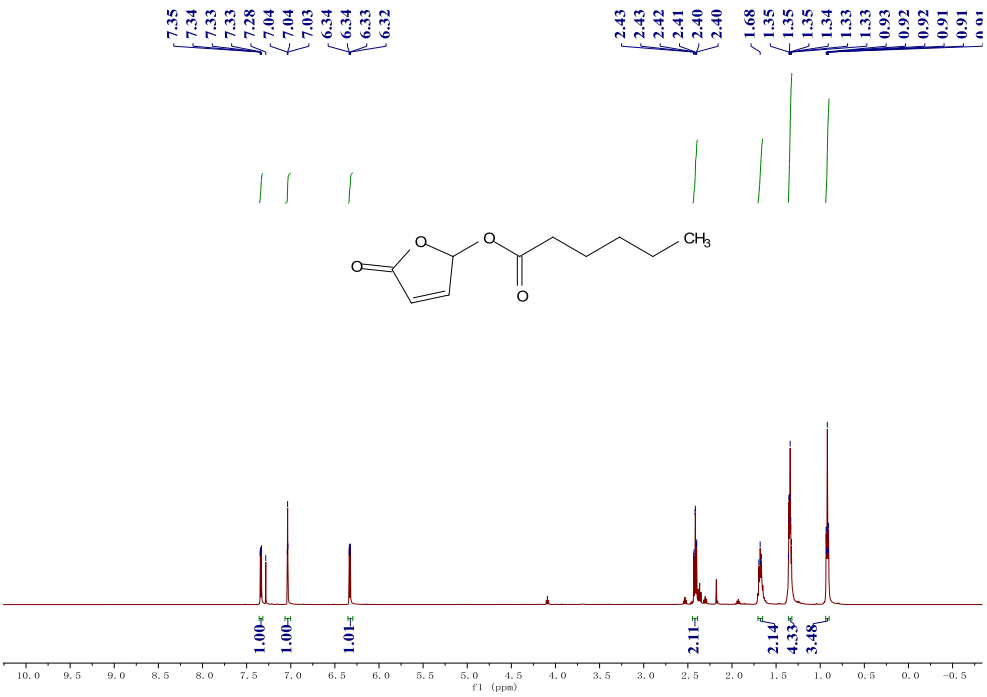

Fig. S19. ^{1}H NMR spectrum of **4c** (500 MHz, $CDCl_3$)

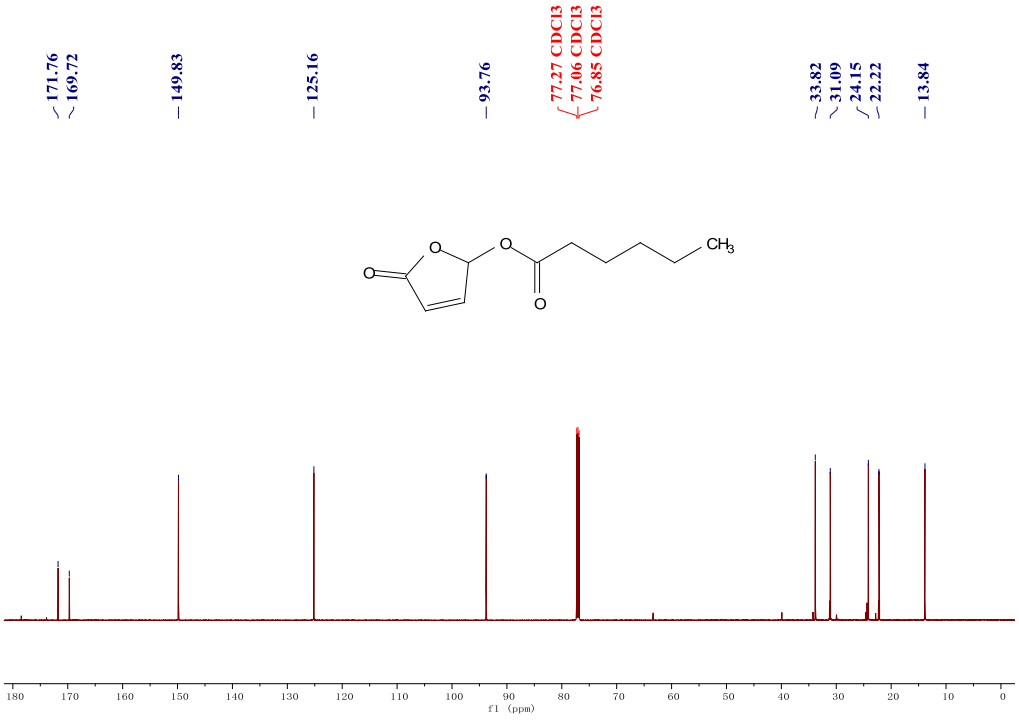

Fig. S20. ^{13}C NMR spectrum of **4c** (151 MHz, $CDCl_3$)

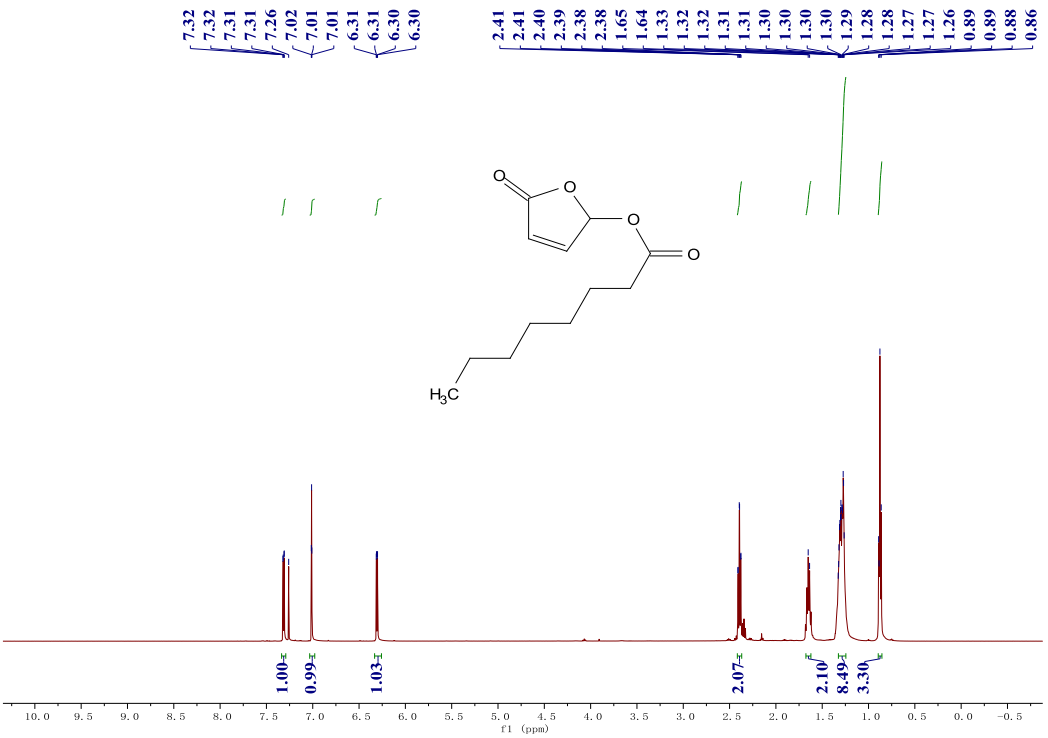

Fig. S21. ^{1}H NMR spectrum of **4d** (500 MHz, $CDCl_3$)

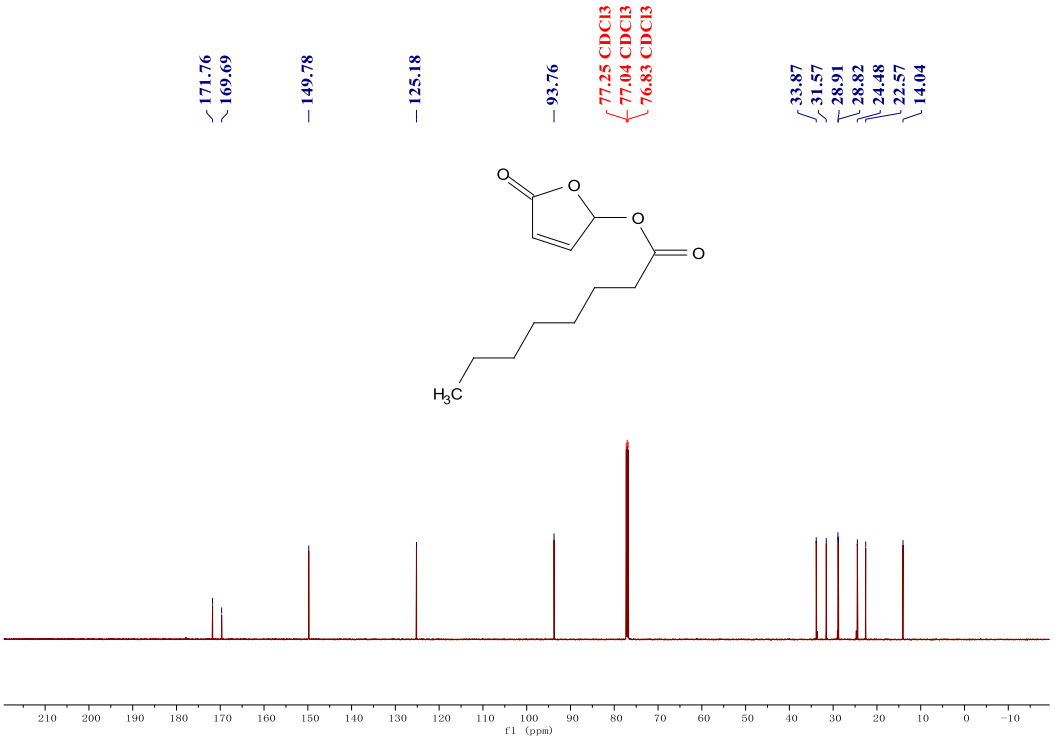

Fig. S22. ^{13}C NMR spectrum of **4d** (151 MHz, $CDCl_3$)

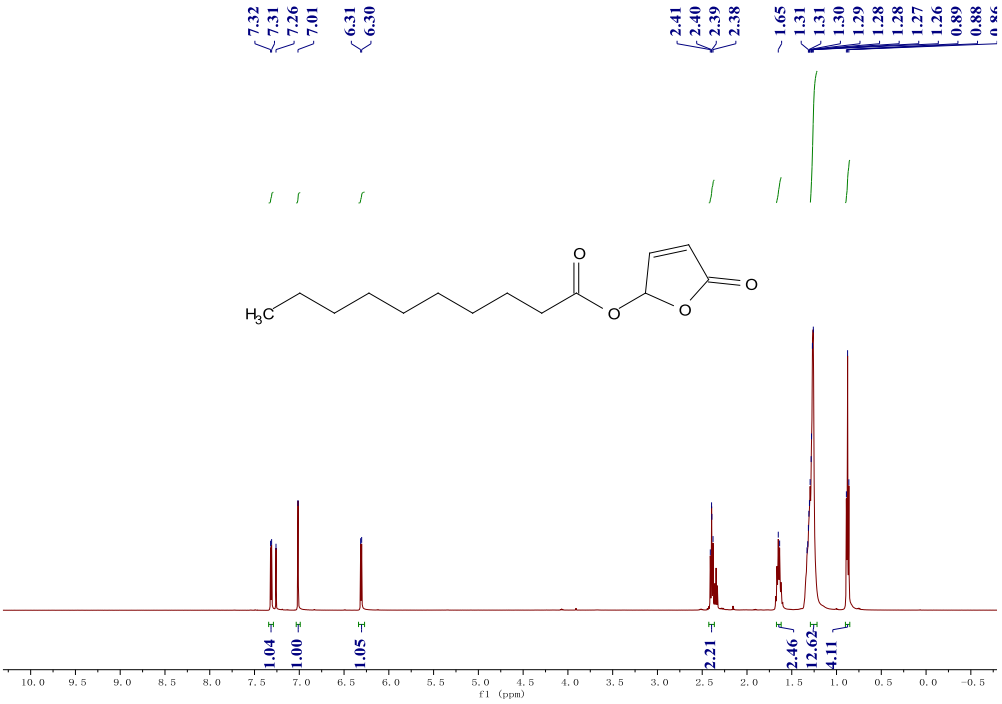

Fig. S23. ^{1}H NMR spectrum of **4e** (500 MHz, $CDCl_3$)

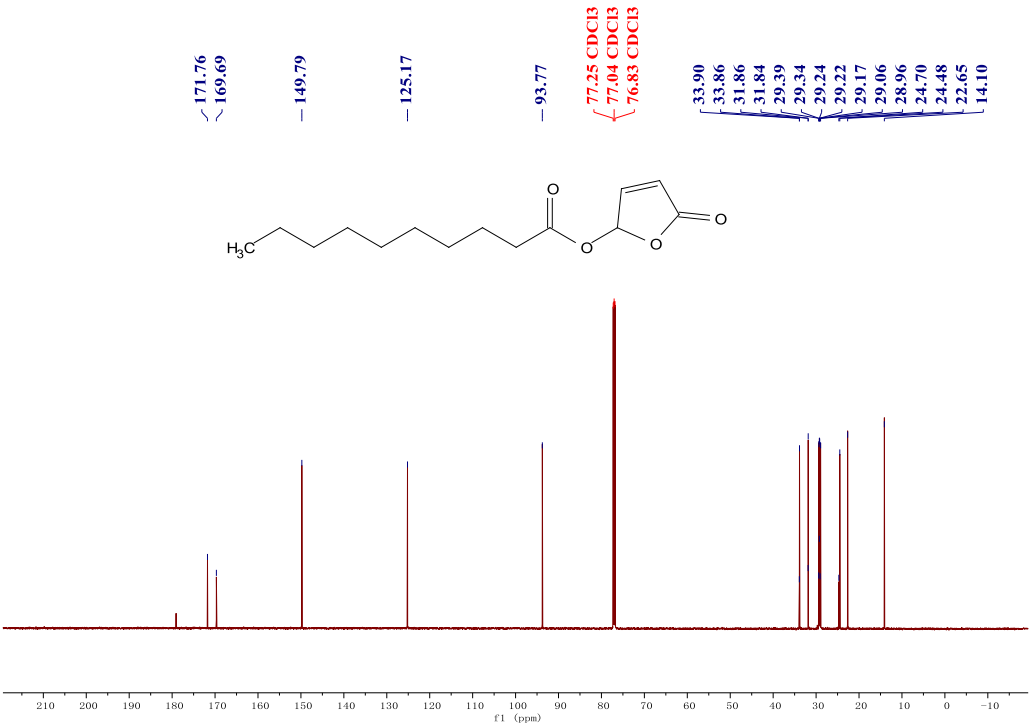

Fig. S24. ^{13}C NMR spectrum of **4e** (151 MHz, $CDCl_3$)

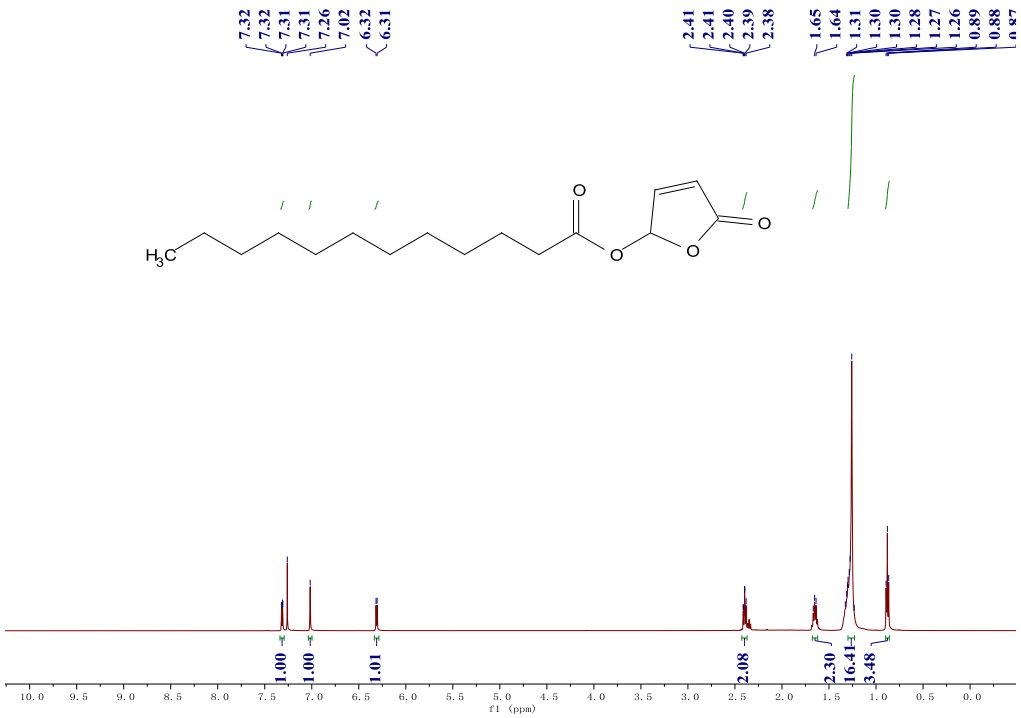

Fig. S25. ^{1}H NMR spectrum of **4f** (500 MHz, $CDCl_3$)

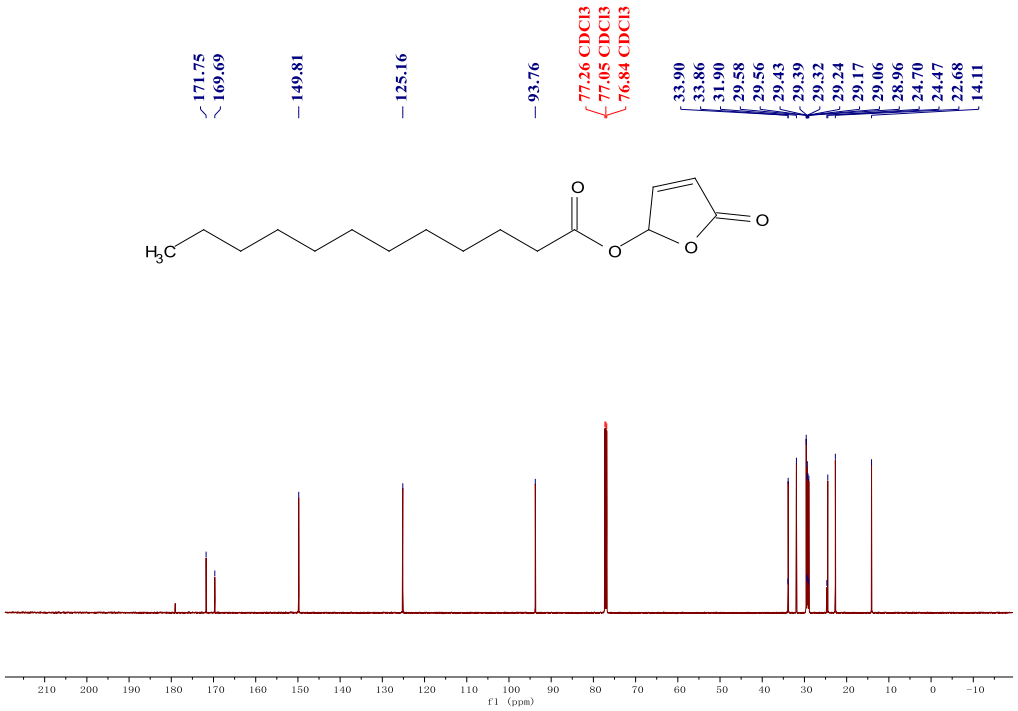

Fig. S26. ^{13}C NMR spectrum of **4f** (151 MHz, $CDCl_3$)

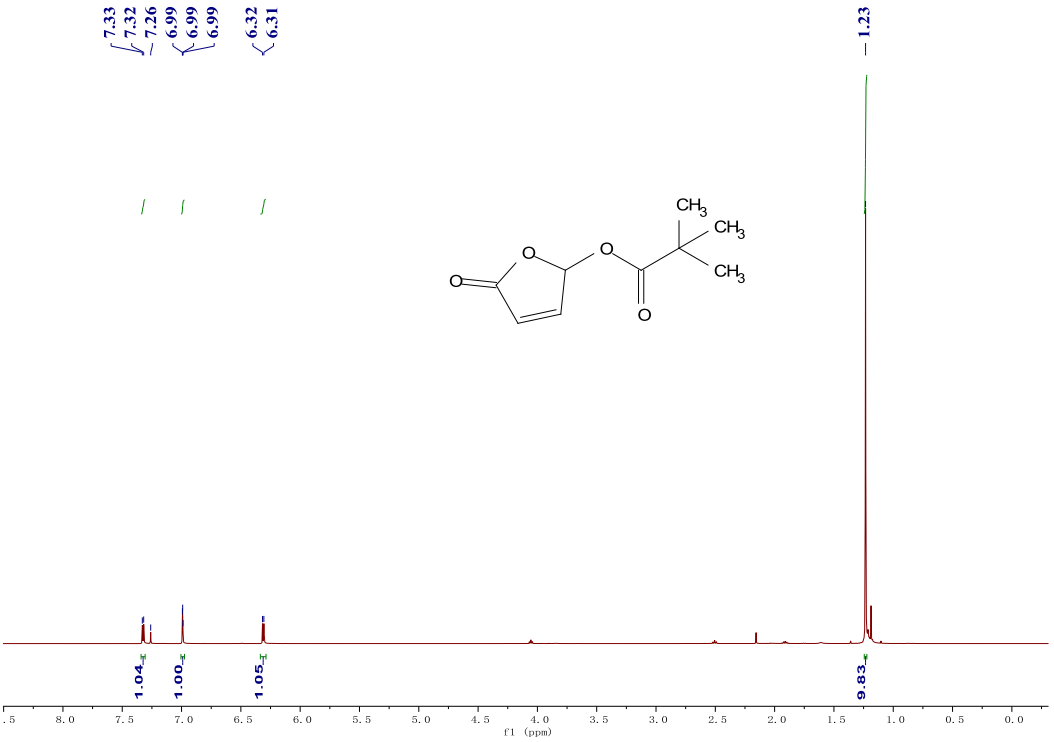

Fig. S27. ^{1}H NMR spectrum of **4g** (500 MHz, $CDCl_3$)

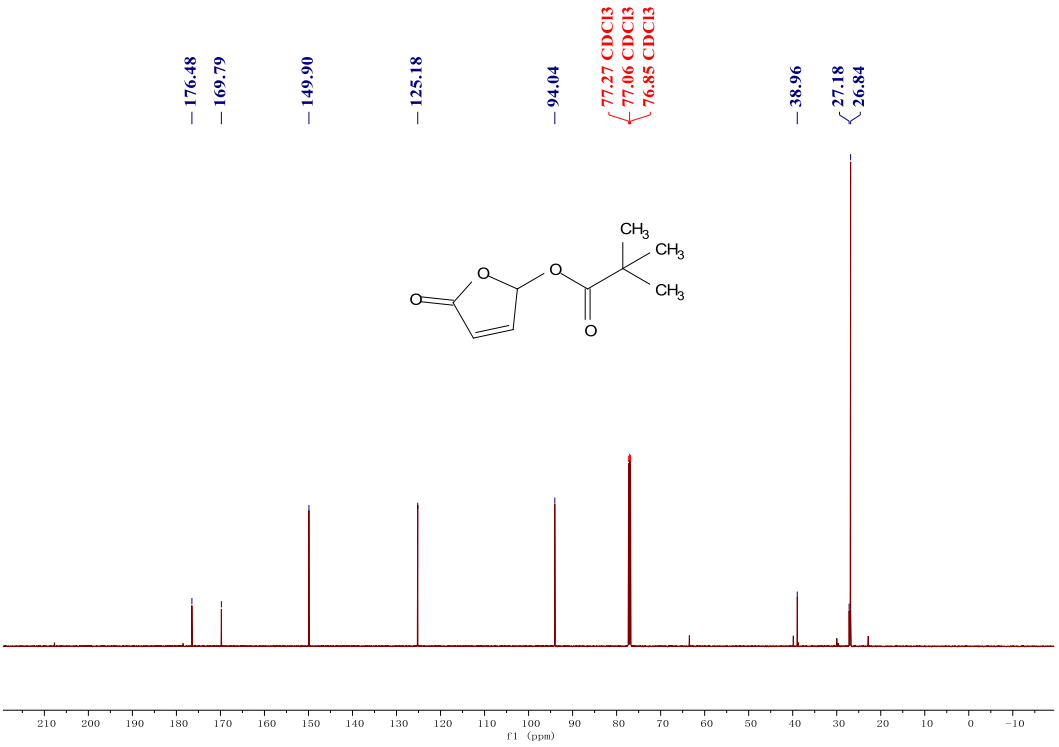

Fig. S28. ^{13}C NMR spectrum of **4g** (151 MHz, $CDCl_3$)

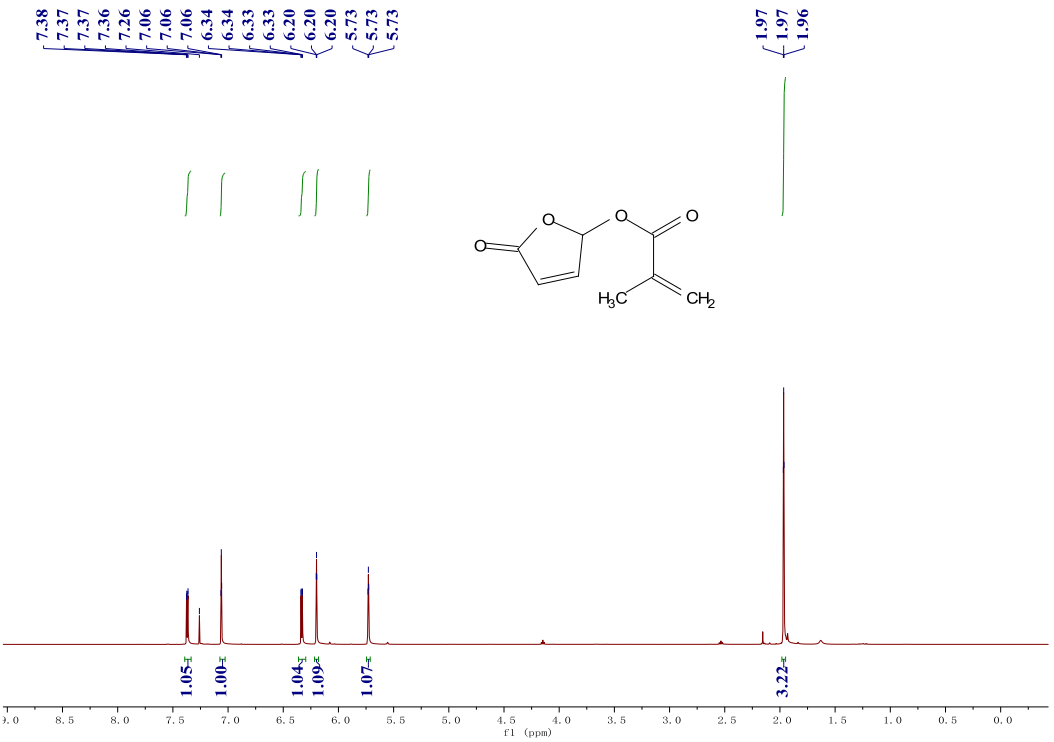

Fig. S29. ^{1}H NMR spectrum of **4h** (500 MHz, $CDCl_3$)

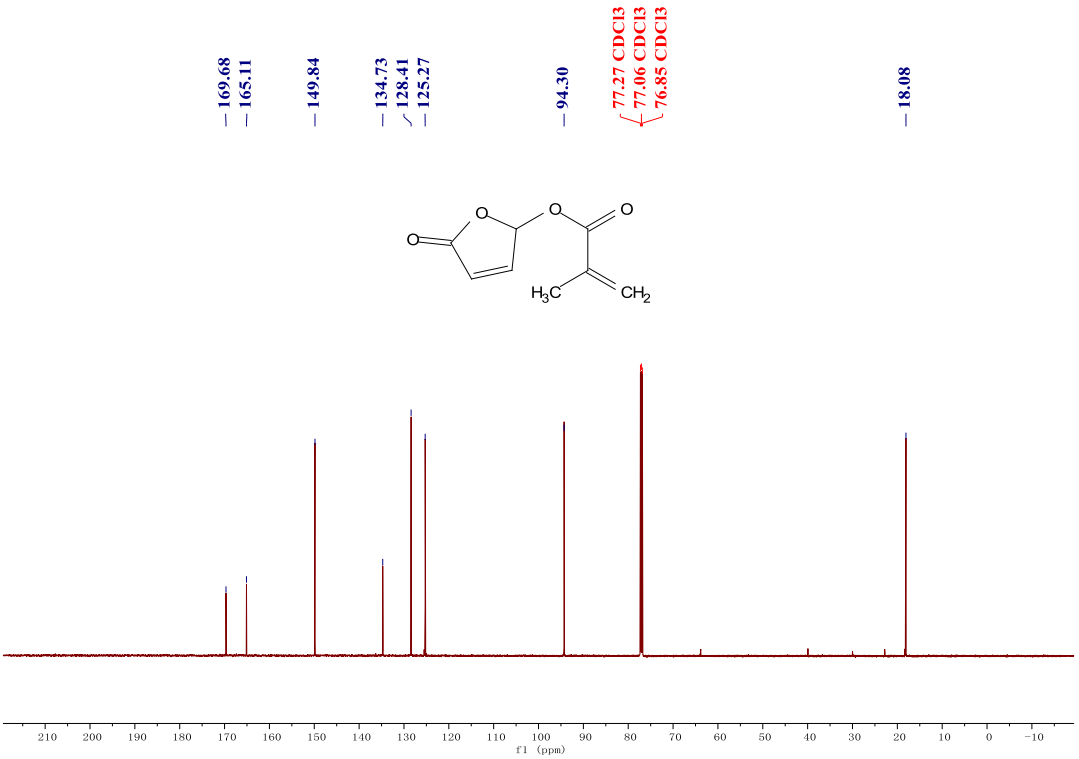

Fig. S30. ^{13}C NMR spectrum of **4h** (151 MHz, $CDCl_3$)

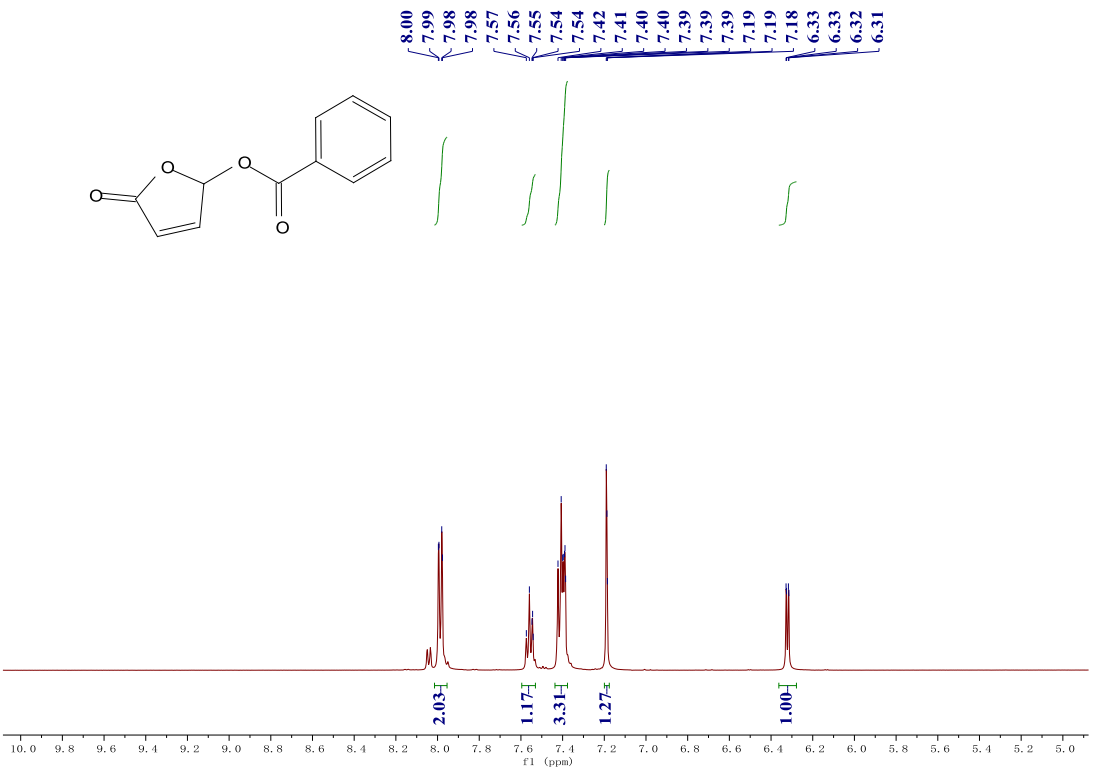

Fig. S31. ^{1}H NMR spectrum of **4i** (500 MHz, $CDCl_3$)

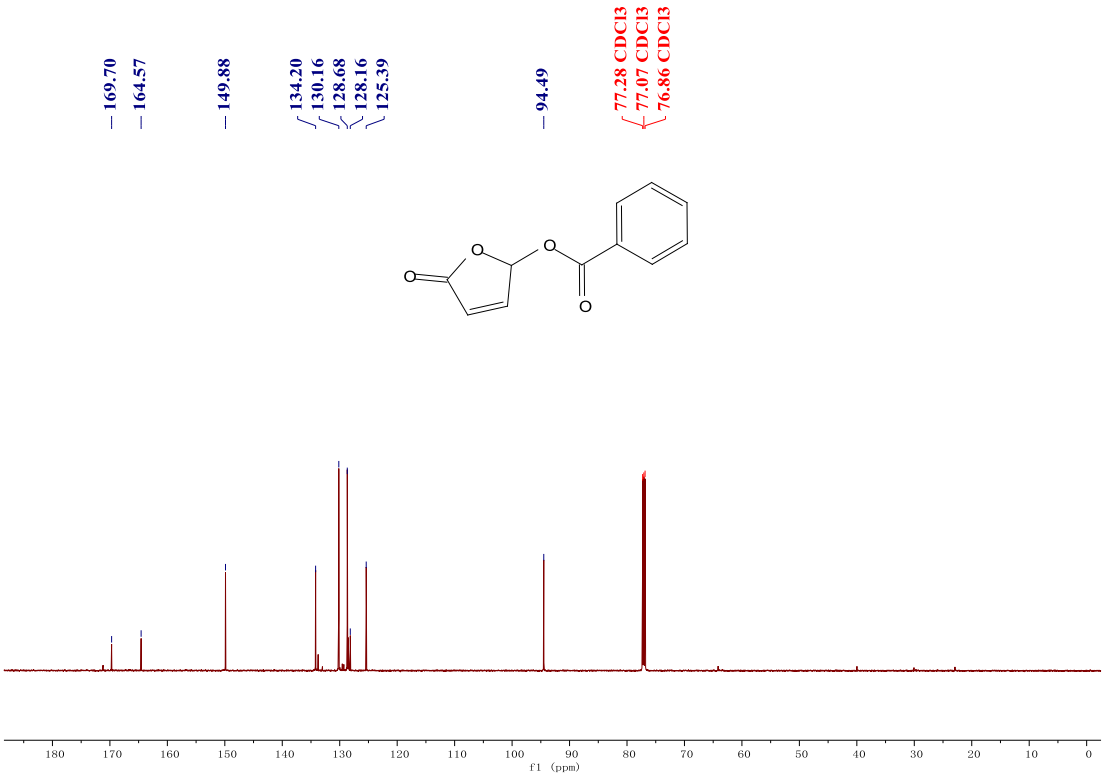

Fig. S32. ^{13}C NMR spectrum of **4i** (151 MHz, $CDCl_3$)

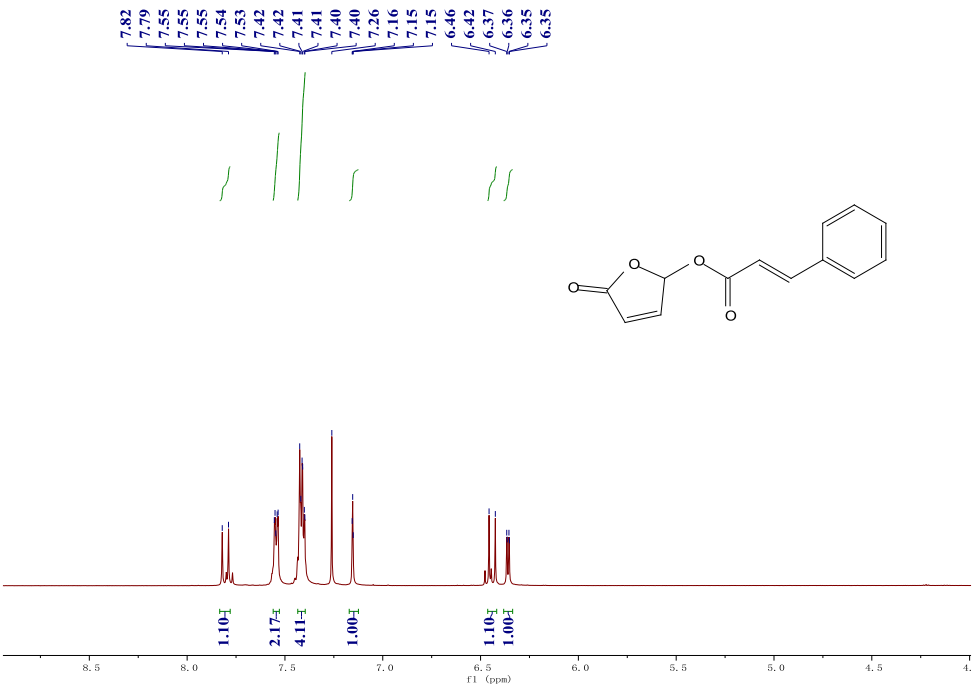

Fig. S33. ^{1}H NMR spectrum of **4j** (500 MHz, $CDCl_3$)

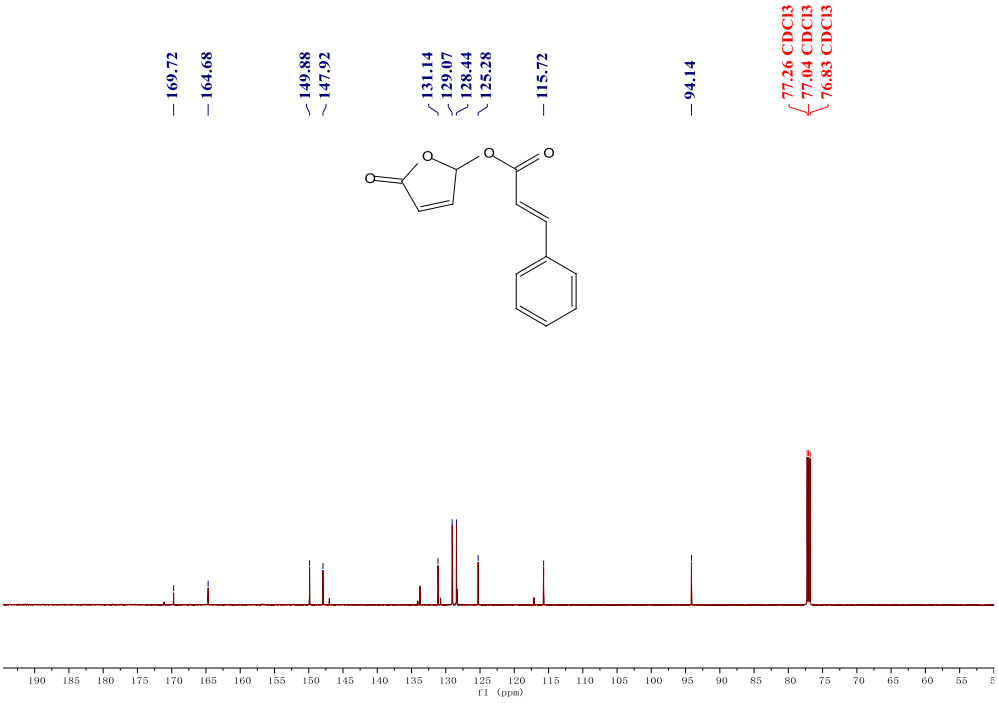

Fig. S34. ^{13}C NMR spectrum of **4j** (151 MHz, $CDCl_3$)

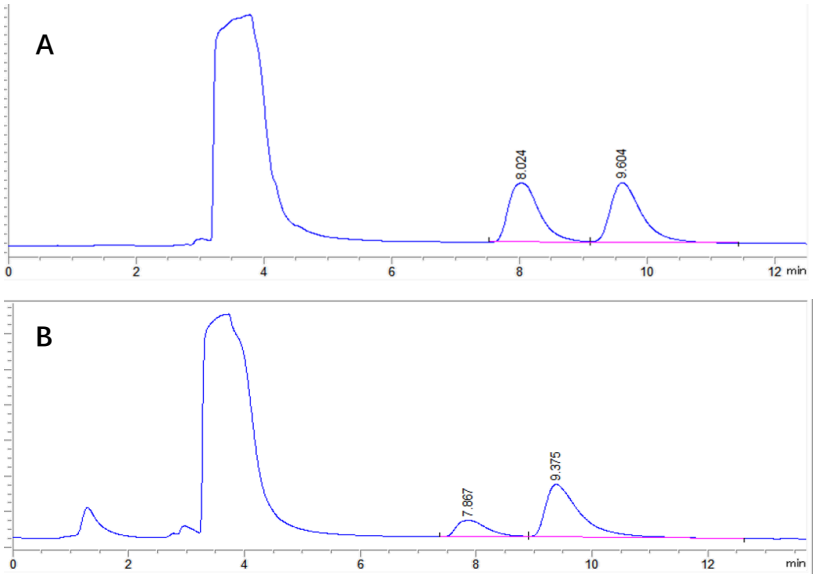

Retention time (min)	Area	Area percent (%)
8.024	11051	49.42
9.604	11310	50.58

Retention time (min)	Area	Area percent (%)
7.867	3559	21.87
9.375	12719	78.13

Fig. S35. Chiral analysis of **4b** synthesized by chemical method (A) and Lipozyme TL IM (B).

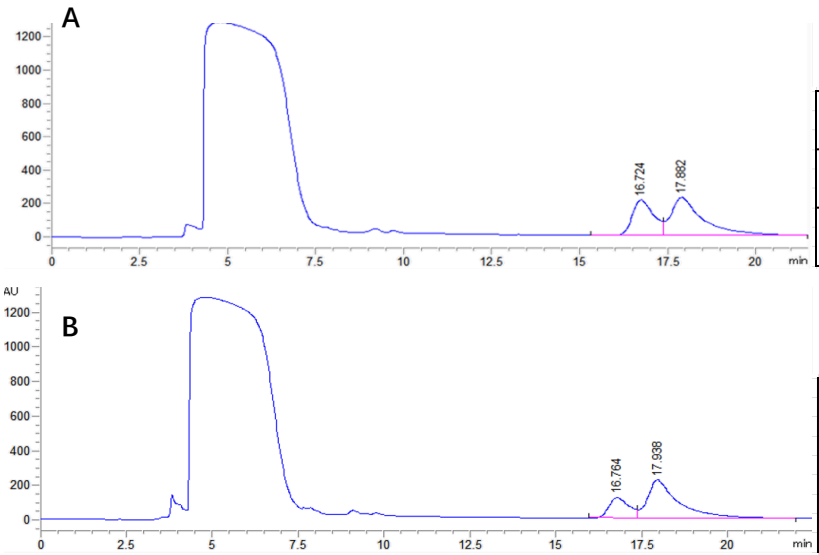

Retention time (min)	Area	Area percent (%)
16.724	8984	38.24
17.882	14512	61.76

Retention time (min)	Area	Area percent (%)
16.764	4846	25.68
17.938	14021	74.32

Fig. S36. Chiral analysis of **4c** synthesized by chemical method (A) and Lipozyme TL IM (B).

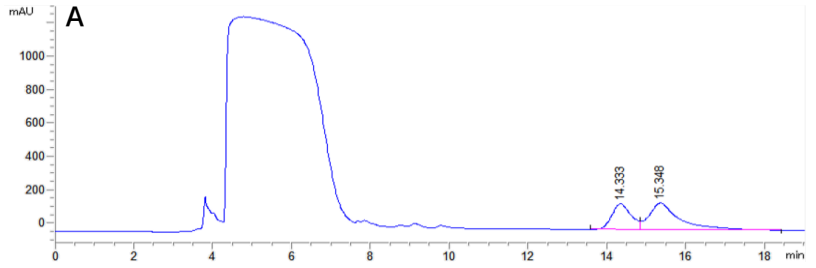

Retention time (min)	Area	Area percent (%)
14.333	5293	38.05
15.348	8617	61.95

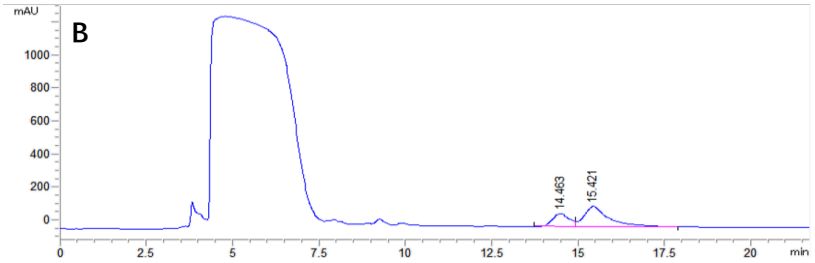

Retention time (min)	Area	Area percent (%)
14.463	2689	30.49
15.421	6132	69.51

Fig. S37. Chiral analysis of **4d** synthesized by chemical method (A) and Lipozyme TL IM (B).

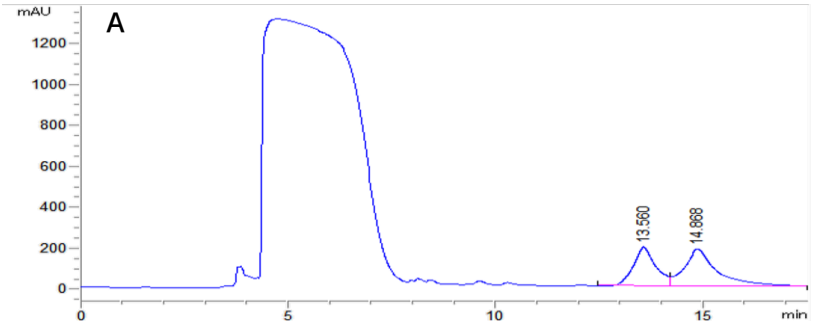

Retention time (min)	Area	Area percent (%)
13.56	7288	42.55
14.868	9838	57.45

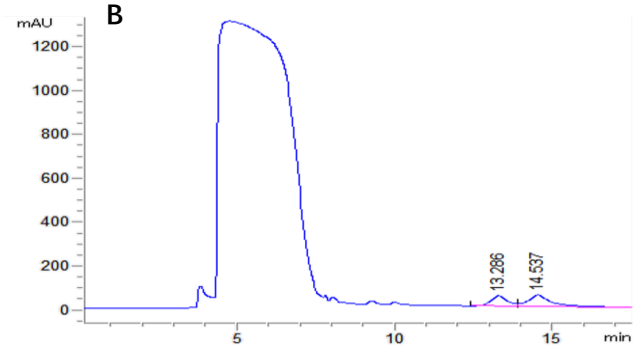

Retention time (min)	Area	Area percent (%)
13.286	1704	38.44
14.537	2729	61.56

Fig. S38. Chiral analysis of **4e** synthesized by chemical method (A) and Lipozyme TL IM (B).

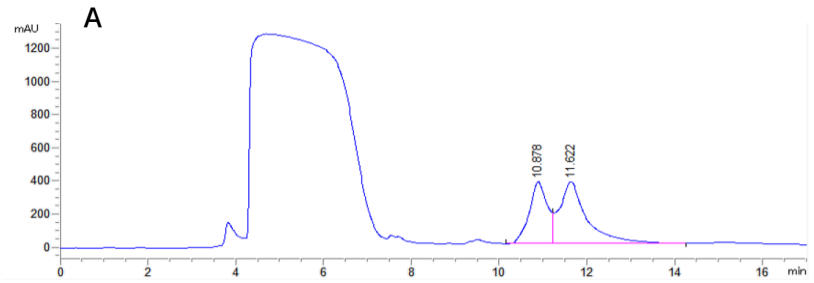

Retention time (min)	Area	Area percent (%)
10.878	10872	40.68
11.622	15916	59.42

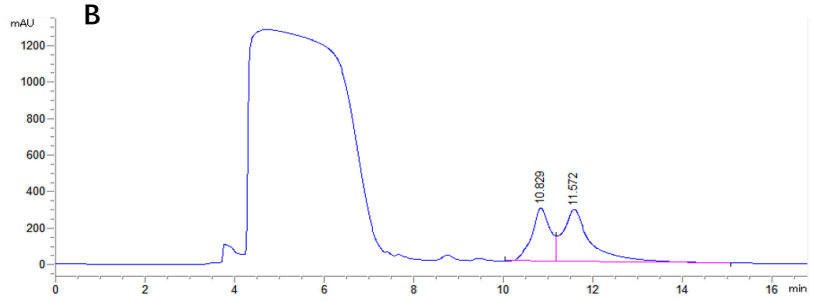

Retention time (min)	Area	Area percent (%)
10.829	8371	40.53
11.572	12284	59.47

Fig. S39. Chiral analysis of **4f** synthesized by chemical method (A) and Lipozyme TL IM (B).

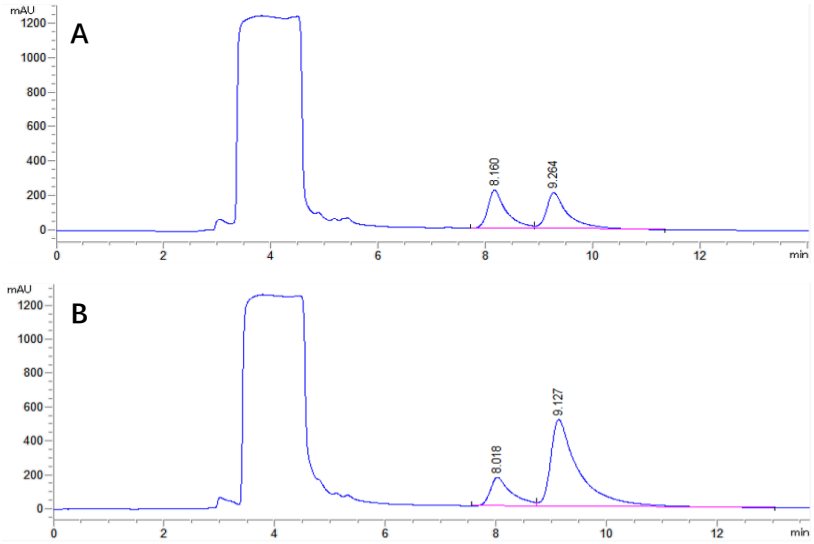

Retention time (min)	Area	Area percent (%)
8.16	5351	47.42
9.264	5933	52.58

Retention time (min)	Area	Area percent (%)
8.018	4579	20.04
9.127	18272	79.96

Fig. S40. Chiral analysis of **4g** synthesized by chemical method (A) and Lipozyme TL IM (B).

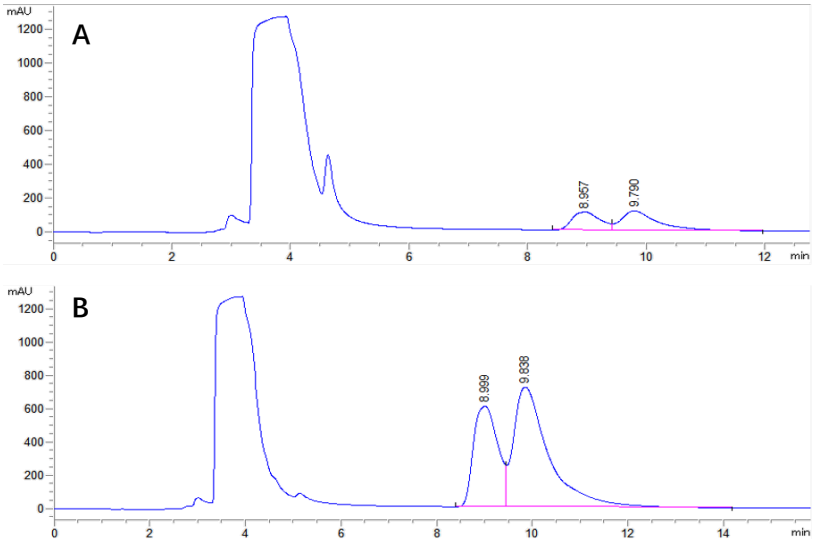

Retention time (min)	Area	Area percent (%)
8.957	3534	41.97
9.264	4886	58.03

Retention time (min)	Area	Area percent (%)
8.999	21305	36.58
9.838	36934	63.42

Fig. S41. Chiral analysis of **4h** synthesized by chemical method (A) and Lipozyme TL IM (B).

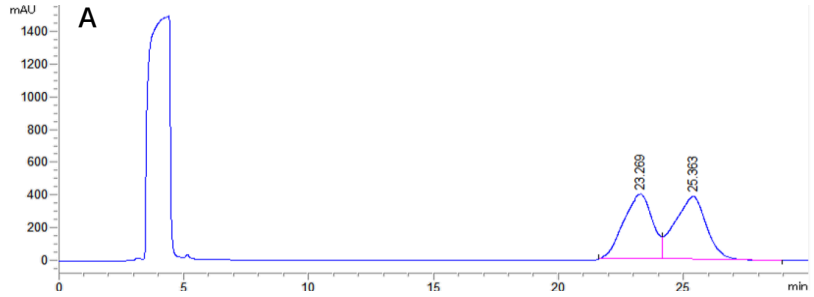

Retention time (min)	Area	Area percent (%)
23.269	32562	49.25
25.363	33559	50.75

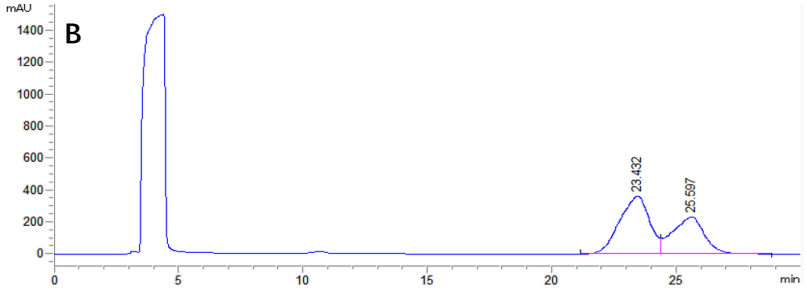

Retention time (min)	Area	Area percent (%)
23.432	30506	60.01
25.593	20328	39.99

Fig. S42. Chiral analysis of **4i** synthesized by chemical method (A) and Lipozyme TL IM (B).

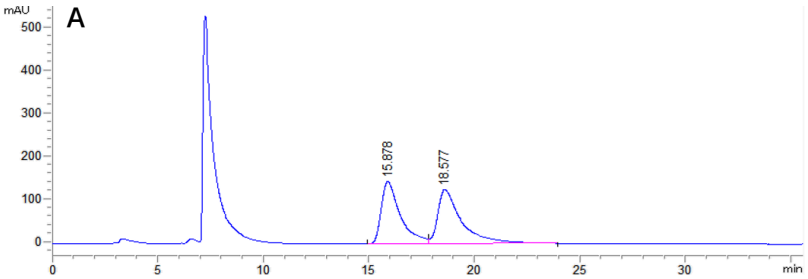

Retention time (min)	Area	Area percent (%)
15.878	9151	48.01
25.363	9913	51.99

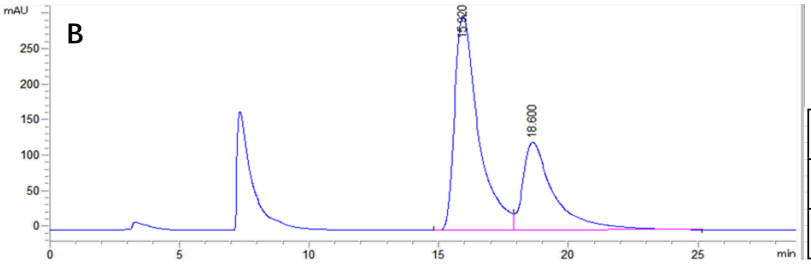

Retention time (min)	Area	Area percent (%)
15.92	19309	65.11
18.6	10347	34.89

Fig. S43. Chiral analysis of **4j** synthesized by chemical method (A) and Lipozyme TL IM (B).

HRMS

Single Mass Analysis
Tolerance = 5.0 mDa / DBE: min = -1.5, max = 50.0
Element prediction: Off
Number of isotope peaks used for i-FIT = 3

Monoisotopic Mass, Even Electron Ions
190 formula(e) evaluated with 1 results within limits (up to 50 best isotopic matches for each mass)
Elements Used:
C: 10-10 H: 14-14 N: 0-100 O: 0-100 Na: 0-1
21
260101-6-4C 11 (0.083)

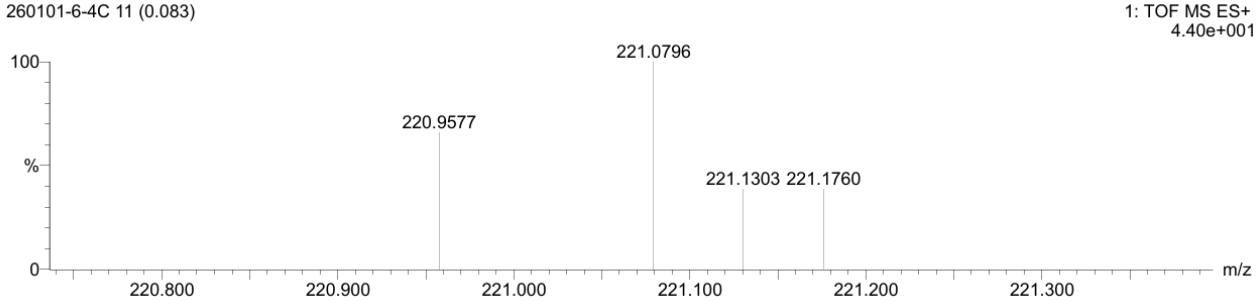

Minimum:				-1.5				
Maximum:		5.0	10.0	50.0				
Mass	Calc. Mass	mDa	PPM	DBE	i-FIT	Norm	Conf(%)	Formula
221.0796	221.0790	0.6	2.7	3.5	24.2	n/a	n/a	C10 H14 O4 Na

Fig. S44. HRMS spectrum of **4c**

Single Mass Analysis
Tolerance = 5.0 mDa / DBE: min = -1.5, max = 50.0
Element prediction: Off
Number of isotope peaks used for i-FIT = 3

Monoisotopic Mass, Even Electron Ions
208 formula(e) evaluated with 1 results within limits (up to 50 best isotopic matches for each mass)
Elements Used:
C: 12-12 H: 19-19 N: 0-100 O: 0-100 Na: 0-1
21
260101-6-4D 13 (0.093)

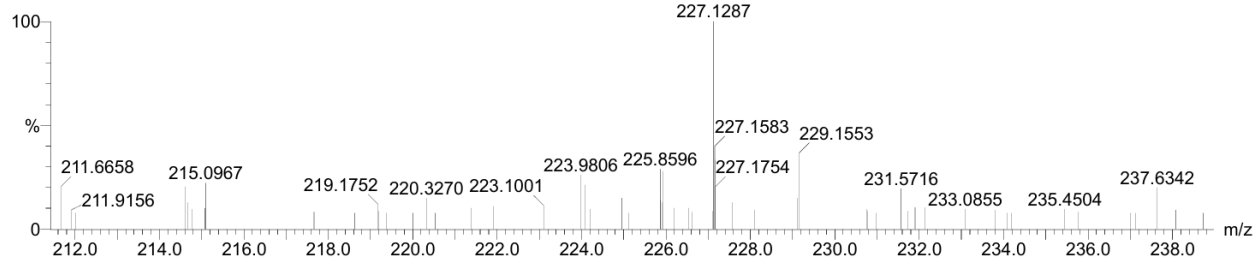

Minimum:				-1.5				
Maximum:		5.0	10.0	50.0				
Mass	Calc. Mass	mDa	PPM	DBE	i-FIT	Norm	Conf(%)	Formula
227.1287	227.1283	0.4	1.8	3.5	60.2	n/a	n/a	C12 H19 O4

Fig. S45. HRMS spectrum of **4d**

Single Mass Analysis
Tolerance = 5.0 mDa / DBE: min = -1.5, max = 50.0
Element prediction: Off
Number of isotope peaks used for i-FIT = 3

Monoisotopic Mass, Even Electron Ions
573 formula(e) evaluated with 1 results within limits (up to 50 best isotopic matches for each mass)
Elements Used:
C: 14-14 H: 22-922 N: 0-100 O: 0-100 Na: 0-1 K: 0-1

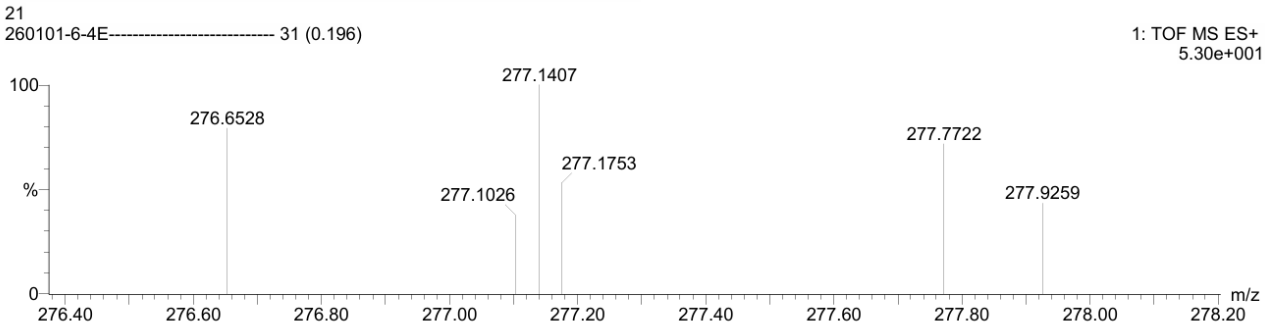

Minimum:				-1.5				
Maximum:		5.0	10.0	50.0				
Mass	Calc. Mass	mDa	PPM	DBE	i-FIT	Norm	Conf(%)	Formula
277.1407	277.1416	-0.9	-3.2	3.5	35.1	n/a	n/a	C14 H22 O4 Na

Fig. S46. HRMS spectrum of **4e**

Single Mass Analysis
Tolerance = 5.0 mDa / DBE: min = -1.5, max = 50.0
Element prediction: Off
Number of isotope peaks used for i-FIT = 3

Monoisotopic Mass, Even Electron Ions
259 formula(e) evaluated with 1 results within limits (up to 50 best isotopic matches for each mass)
Elements Used:
C: 13-13 H: 10-10 N: 0-100 O: 0-100 Na: 0-1

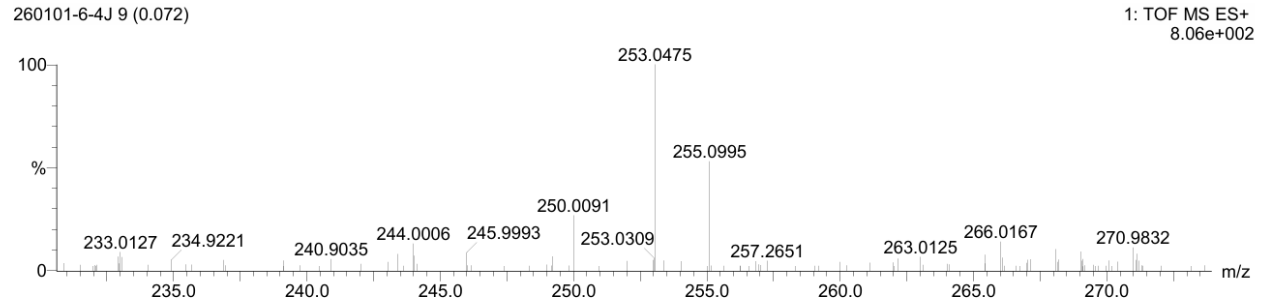

Minimum:				-1.5				
Maximum:		5.0	10.0	50.0				
Mass	Calc. Mass	mDa	PPM	DBE	i-FIT	Norm	Conf(%)	Formula
253.0475	253.0477	-0.2	-0.8	8.5	47.2	n/a	n/a	C13 H10 O4 Na

Fig. S47. HRMS spectrum of **4j**

HPLC calibration curves

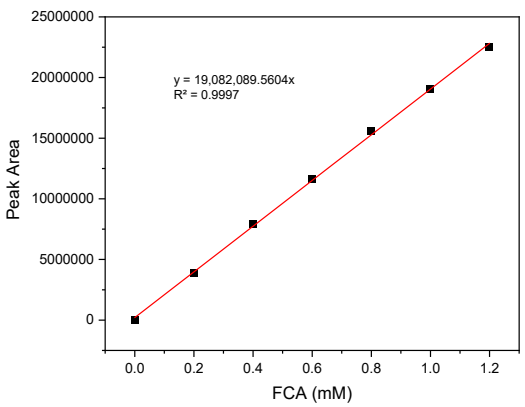

Calibration curve of FCA

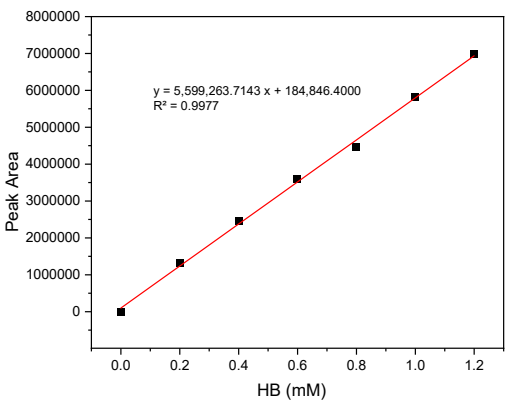

Calibration curve of HB

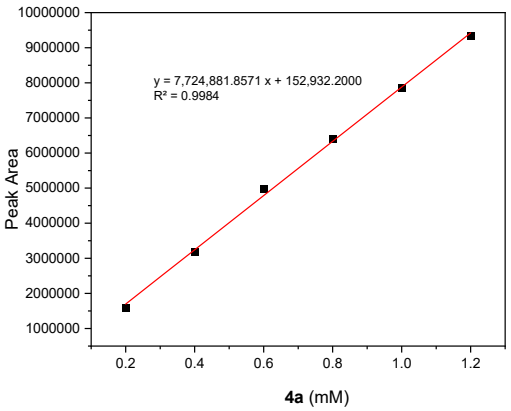

Calibration curve of **4a**

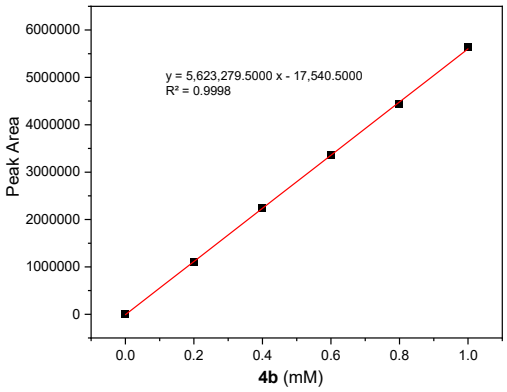

Calibration curve of **4b**

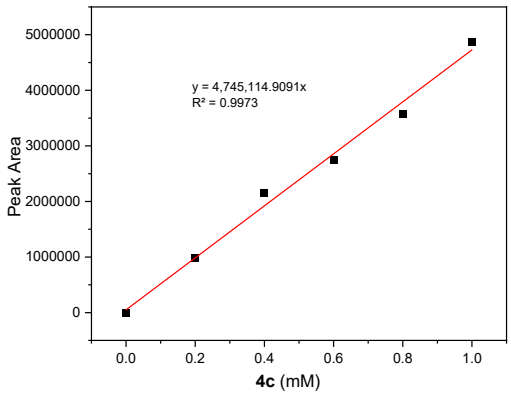

Calibration curve of **4c**

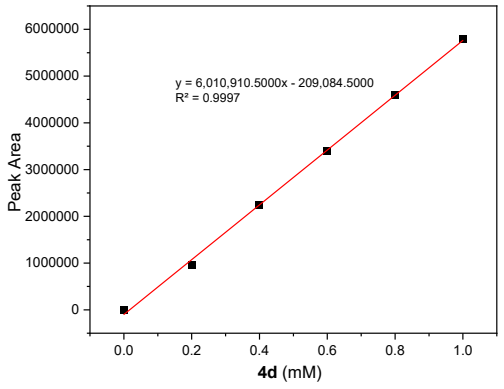

Calibration curve of **4d**

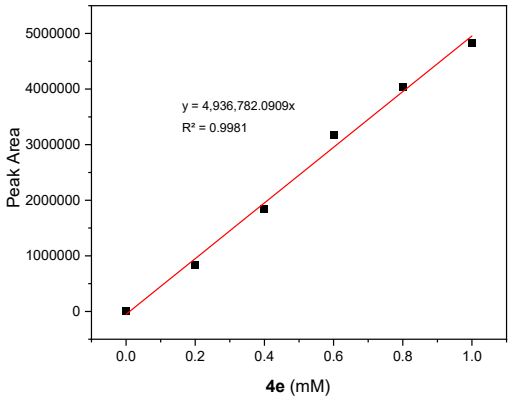

Calibration curve of **4e**

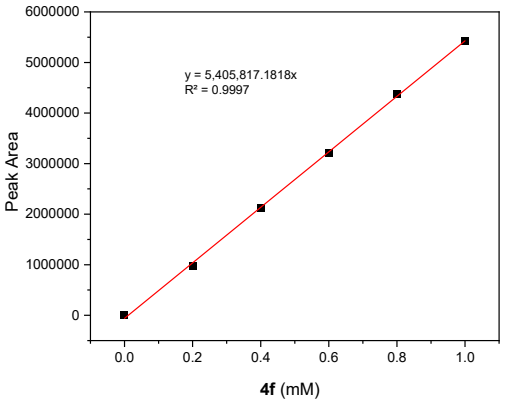

Calibration curve of **4f**

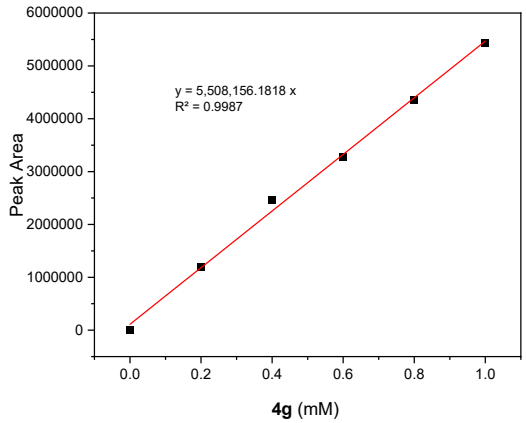

Calibration curve of **4g**

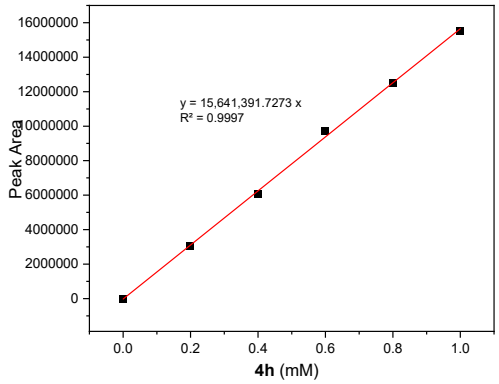

Calibration curve of **4h**

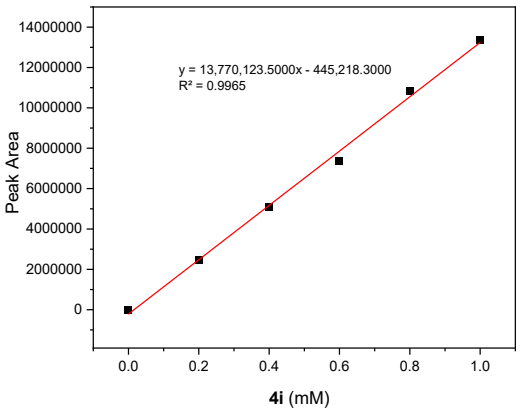

Calibration curve of **4i**

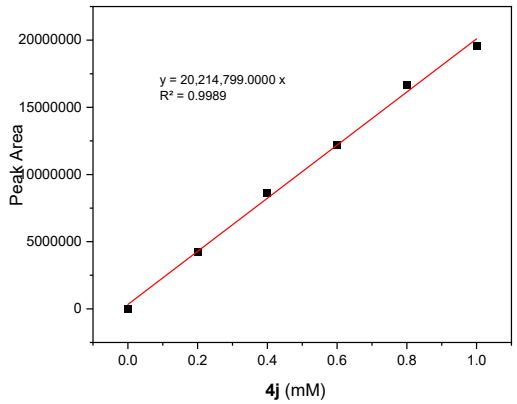

Calibration curve of **4j**

References

1. M. L. Lepage, G. Alachouzos, J. G. H. Hermens, N. Elders, K. J. van den Berg and B. L. Feringa, *J. Am. Chem. Soc.*, 2023, **145**, 17211–17219.
2. H. van der Deen, A. D. Cuiper, R. P. Hof, A. van Oeveren, B. L. Feringa and R. M. Kellogg, *J. Am. Chem. Soc.*, 1996, **118**, 3801–3803.
3. D. Feng, Z.-Y. Gu, J.-R. Li, H.-L. Jiang, Z. Wei and H.-C. Zhou, *Angew. Chem. Int. Ed.*, 2012, **51**, 10307–10310.
4. D. Feng, W.-C. Chung, Z. Wei, Z.-Y. Gu, H.-L. Jiang, Y.-P. Chen, D. J. Darensbourg and H.-C. Zhou, *J. Am. Chem. Soc.*, 2013, **135**, 17105–17110.
5. K. Mao, Y. Zhu, J. Rong, F. Qiu, H. Chen, J. Xu, D. Yang, T. Zhang and L. Zhong, *Colloids Surf., A*, 2021, **611**, 125888.
6. X.-L. Ma, L.-H. Ma, S. Guo, Z.-M. Zhang and T.-B. Lu, *Angew. Chem. Int. Ed.*, 2025, **64**, e202423157.
7. G. Nardi, I. Manet, S. Monti, M. A. Miranda and V. Lhiaubet-Vallet, *Free Radicals Biol. Med.*, 2014, **77**, 64–70.
8. T. Takajo, Y. Kurihara, K. Iwase, D. Miyake, K. Tsuchida and K. Anzai, *Chem. Pharm. Bull.*, 2020, **68**, 150–154.